UNLIMITED
UNCLASSIFIED

Canada

④

AN IMPROVED AIRBORNE WIND MEASUREMENT TECHNIQUE FOR THE NAE TWIN OTTER

DTIC
S ELECTE
FEB 0 9 1990
B D

by

B.W. Leach and J.I. MacPherson

National Aeronautical Establishment

OTTAWA
NOVEMBER 1989

AERONAUTICAL NOTE
NAE-AN-61
NRC NO. 31023

National Research
Council Canada

Conseil national
de recherches Canada

NATIONAL AERONAUTICAL ESTABLISHMENT

SCIENTIFIC AND TECHNICAL PUBLICATIONS

AERONAUTICAL REPORTS

Aeronautical Reports (LR): Scientific and technical information pertaining to aeronautics considered important, complete, and a lasting contribution to existing knowledge.

Mechanical Engineering Reports (MS): Scientific and technical information pertaining to investigations outside aeronautics considered important, complete, and a lasting contribution to existing knowledge.

AERONAUTICAL NOTES (AN): Information less broad in scope but nevertheless of importance as a contribution to existing knowledge.

LABORATORY TECHNICAL REPORTS (LTR): Information receiving limited distribution because of preliminary data, security classification, proprietary, or other reaons.

Details on the availability of these publications may be obtained from:

Graphics Section,
National Research Council Canada,
National Aeronautical Establishment,
Bldg. M-16, Room 204,
Montreal Road,
Ottawa, Ontario
K1A 0R6

ÉTABLISSEMENT NATIONAL D'AÉRONAUTIQUE

PUBLICATIONS SCIENTIFIQUES ET TECHNIQUES

RAPPORTS D'AÉRONAUTIQUE

Rapports d'aéronautique (LR): Informations scientifiques et techniques touchant l'aéronautique jugées importantes, complètes et durables en termes de contribution aux connaissances actuelles.

Rapports de génie mécanique (MS): Informations scientifiques et techniques sur la recherche externe à l'aéronautique jugées importantes, complètes et durables en termes de contribution aux connaissances actuelles.

CAHIERS D'AÉRONAUTIQUE (AN): Informations de moindre portée mais importantes en termes d'accroissement des connaissances.

RAPPORTS TECHNIQUES DE LABORATOIRE (LTR): Informations peu disséminées pour des raisons d'usage secret, de droit de propriété ou autres ou parce qu'elles constituent des données préliminaires.

Les publications ci-dessus peuvent être obtenues à l'adresse suivante:

Section des graphiques,
Conseil national de recherches Canada,
Établissement national d'aéronautique,
Im. M-16, pièce 204,
Chemin de Montréal,
Ottawa (Ontario)
K1A 0R6

AN IMPROVED AIRBORNE WIND MEASUREMENT TECHNIQUE FOR THE NAE TWIN OTTER

NOUVELLE MÉTHODE DE MESURE DU VENT EN VOL À BORD DU TWIN OTTER DE L'ÉNA

by/par

B.W. Leach and J.I. MacPherson

National Aeronautical Establishment

S.R.M. Sinclair, Head/Chef
Flight Research Laboratory/
Laboratoire de recherches en vol
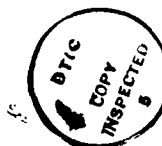
G.F. Marsters
Director/directeur

AN IMPROVED AIRBORNE WIND MEASUREMENT
TECHNIQUE FOR THE NAE TWIN OTTER

SUMMARY

Airborne wind measurement techniques currently being used onboard the NAE Twin Otter Atmospheric Research Aircraft are described and their fundamental limitations are discussed. In particular, a recently acquired LTN-90-100 strapdown inertial reference system (IRS) demonstrates significant low frequency Schuler oscillations in its velocity components (attaining peak errors of 2 to 3 mps), actually degrading wind computation accuracy compared with older techniques. A new wind measurement technique, based on a Kalman filter integrated navigation approach, is described which solves this problem and provides wind computation accuracy superior to previous methods. Preliminary results, based on applying the Kalman filter to Twin Otter flight test data, indicate that inertial velocity accuracies of 0.3 mps RMS (per channel) are attainable, with a corresponding improvement in the accuracy of earth-referenced wind components.

RÉSUMÉ

On trouvera une description des méthodes de mesure du vent en vol acutellement utilisées à bord du Twin Otter de l'ÉNA chargé des recherches atmosphériques ainsi qu'une discussion portant sur les limites fondamentales de ces méthodes. En particulier, le système inertial de référence (IRS) à composants liés LTN-90-100 acquis récemment est sujet à d'importantes oscillations de Schuler à basse fréquence (les erreurs peuvent atteindre 2 à 3 mps), ce qui se traduit par des calculs du vent moins exacts qu'à l'aide des anciennes méthodes. On trouvera une description d'une nouvelle méthode de mesure du vent qui repose sur une navigation intégrée à filtre de Kalman, laquelle résout ce problème et permet de mesurer le vent avec une exactitude supérieure à celle des anciennes méthodes. D'après les premiers résultats basés sur l'application d'un filtre de Kalman aux données des essais en vol du Twin Otter, il semble qu'il soit possible d'obtenir une déviation standard de 0,3 mps (par canal) pour la vitesse inertielle et une amélioration semblable aux composants de la vitesse du vent mesurés par rapport au sol.

CONTENTS

TABLES

ILLUSTRATIONS

AN IMPROVED AIRBORNE WIND MEASUREMENT
TECHNIQUE FOR THE NAE TWIN OTTER

1.0   INTRODUCTION

The NAE Twin Otter Atmospheric Research Aircraft was first instrumented for air motion measurement in 1980 and has undergone continual instrumentation development since then. The recent acquisition of a Litton LTN-90-100 inertial reference system (IRS), supplemented by the existing Doppler velocity sensor and airborne Loran-C positioning receiver, has sparked an interest in developing an integrated navigation system approach onboard the aircraft. A Kalman filter navigator would improve the accuracy of position and velocity sensing and, most importantly, airborne wind measurement.

Section 2 briefly describes the hardware presently onboard the Twin Otter for both inertial navigation and air data sensing. In Section 3, three relatively standard wind computation techniques currently implemented onboard the Twin Otter are described, and the fundamental limitations of each method are clearly shown using flight data from the field. Of primary concern is the fact that a modern, state-of-the-art strapdown IRS still does not produce inertial velocities with the accuracy required for proper wind computation. This fact is well documented in Section 3 using wind data from the 1988 Eulerian Model Evaluation Field Study (EMEFS) project, where slowly varying IRS velocity errors with peak magnitudes of 2 to 3 meters per second (mps) were routinely observed.

Section 4 provides details of a Kalman filter integrated navigation algorithm that has been designed specifically for the navigation sensor configuration onboard the Twin Otter. This sophisticated approach to real-time navigation involves the optimal blending of navigation data from three sources: a Litton LTN-90-100 IRS, a Decca Type 72 Doppler radar velocity sensor and an ARNAV R-40 airborne Loran-C receiver. In essence, the IRS and Doppler velocity sensor can be continuously calibrated in flight by the Kalman filter, leading to a significant improvement in inertial velocity accuracy for wind computations. The same Kalman filter computer algorithm can also be used in an off-line manner for post-flight wind computations, if desired.

The expected accuracy of this Kalman filter design is demonstrated in Section 5, using representative flight test data from the Twin Otter data acquisition system. The rather significant inertial velocity error levels, inherent to both the unaided IRS and unaided Doppler system, are clearly demonstrated by using Kalman filter analysis techniques, as is the position error buildup in the IRS. It is shown that, in a root mean square (RMS) sense, IRS velocity errors can be reduced to about +/-0.3 mps in each of the three orthogonal components and IRS position errors can be reduced to about +/-0.2 nautical miles (nm) in each of the two horizontal components. Three different Kalman filter processing scenarios are analyzed - 1) Loran-C/IRS only, ii) Doppler/IRS only and iii) Loran-C/Doppler/IRS, providing some rather interesting results. A comparison is then made between wind computations based on Kalman filter-corrected IRS velocities and those computed using the three standard techniques currently available on the Twin Otter, in order to show the consistency of this new approach.

Section 6 summarizes the reasons for utilizing a Kalman filtering technique for airborne wind measurement, the results that have been achieved to date using this approach and future plans for its implementation onboard the NAE Twin Otter aircraft.

2.0   WIND INSTRUMENTATION ONBOARD THE NAE TWIN OTTER

The NAE Twin Otter Atmospheric Research Aircraft has been instrumented to measure the three orthogonal components of atmospheric motion (U_{GE}, V_{GE} and W_{GE}) over a frequency range of 0 to 5 Hz. Details of the present Twin Otter instrumentation for wind measurement will be given in this section. Figure 1 is a diagram of the aircraft, showing the mounting locations of the various instruments involved in wind sensing.

2.1 Air Data Instrumentation

Air motion relative to the aircraft is measured by a nose-mounted gust boom incorporating a Rosemount 858 5-hole probe (see Fig.1). This device, together with the associated pressure transducers, measures static pressure (altitude), dynamic pressure (airspeed) and the angles of attack and sideslip. As well, by employing a total temperature sensor, true airspeed (TAS) can be measured. A second altitude/airspeed system employs a separate set of pressure transducers connected to the fuselage-mounted pitot and static ports used for the flight instruments. Table 2.1 lists the air data sensors installed on the Twin Otter at the present time and Table 2.2 gives their specifications.

TABLE 2.1

TWIN OTTER AIR DATA SENSORS

INSTRUMENT	OUTPUT[1] TYPE	DESCRIPTION
Rosemount 102DJ1CG	A	Fast response total temperature at nose
Paroscientific 215L-AW-012 Rosemount 858AJ28 probe	D	Noseboom static pressure, temperature compensated
Rosemount 12211V7A1B Rosemount 858AJ28 probe	A	Noseboom dynamic pressure
Rosemount 12211F1VL5A1 Rosemount 858AJ28 probe	A	Differential pressure for angle of attack
Rosemount 12211F1VL5A1 Rosemount 858AJ28 probe	A	Differential pressure for angle of sideslip
Rosemount 1201F1B4A1B	A	Alternate static pressure, fuselage
Rosemount 1201F2VL7A1A	A	Alternate dynamic pressure, fuselage

[1] A - Analog   D - Digital

TABLE 2.2

AIR DATA SENSOR SPECIFICATIONS

PARAMETER	UNITS	RESOLUTION	RMS OF CALIBRATION
Total Temperature at Nose	Deg K	2.534×10^{-2}	3.793×10^{-2}
Noseboom Static Pressure	Mb	–	4.839×10^{-2}
Noseboom Dynamic Pressure	Mb	1.124×10^{-2}	1.114×10^{-2}
Angle of Attack Pressure	Mb	2.252×10^{-2}	4.006×10^{-2}
Angle of Sideslip Pressure	Mb	2.402×10^{-2}	7.353×10^{-2}
Fuselage Static Pressure	Mb	2.692×10^{-1}	1.164×10^{-1}
Fuselage Dynamic Pressure	Mb	1.848×10^{-2}	1.928×10^{-2}

2.2 Navigation Instrumentation

The Twin Otter's suite of navigation sensors available for position and velocity sensing is as follows:

I) **Litton LTN-90-100 Inertial Reference System** - this modern, three-axis strapdown inertial system (called an IRS - Inertial Reference System - by Litton) utilizes ring laser gyro technology and a digital data bus (ARINC 429 standard) to provide a set of 24 inertial parameters in digital form, many at a 64 Hz data rate. Table 2.3 gives the specifications for the set of 16 of these IRS parameters recorded by the onboard data acquisition system at a 16 Hz data rate. Table 2.4 lists the fundamental specifications of the system's accelerometers and gyroscopes -- these statistical specifications will be of importance in the Kalman filter design. This particular IRS requires barometric altimeter data, in ARINC 429 format, as an input in order to stabilize the vertical channel. Typical accuracy for this type of IRS is quoted as 1 nm/hr in the horizontal position components and 2.5 mps in the horizontal velocity components (Ref. 1).

II) **Decca Doppler Radar Type 72** - this 3-beam Janus Doppler radar system measures the three body-axis (i.e. U, V, W) components of aircraft velocity (Ref. 2). The NAE-designed interface for this unit is such that each Doppler velocity component is averaged over a 1/2 second interval and then sampled, yielding an effective sample rate of 2 Hz. Table 2.5 gives the specifications for the three Doppler velocity components.

III) **ARNAV R-40-AVA-1000A Loran-C Receiver** - this airborne Loran-C receiver provides digital geographical latitude and longitude data, at a nominal 0.7 Hz update rate, via a standard RS-232C serial output port. Most of the United States, and much of Canada, has Loran-C coverage via a series of Loran-C chains scattered across the continent (Ref. 3). Table 2.5 also provides specifications for the two Loran-C position components that are being sampled.

IV) **NAE Inertial Instrumentation Package** - this is a set of inertial measurement instruments that has been used onboard the aircraft since 1981 for wind calculations. Table 2.6 gives a list of these instruments and Table 2.7 shows their specifications.

TABLE 2.3

DIGITAL DATA PARAMETERS FROM LTN-90-100 IRS

	PARAMETER	UNITS	RESOLUTION	POSITIVE SENSE
1.	Latitude	Degs	0.000172	North From 0°
2.	Longitude	Degs	0.000172	East From 0°
3.	Inertial Altitude	Meters	0.038100	Up
4.	North/South Velocity	M/s	0.064346	North
5.	East/West Velocity	M/s	0.064346	East
6.	Inertial Vertical Speed	M/s	0.005080	Up
7.	Pitch Angle	Degs	0.005493	Up
8.	Roll Angle	Degs	0.005493	Right Wing Down
9.	True Heading	Degs	0.005493	CW From Tr North
10.	Body Pitch Rate	Deg/s	0.003906	Up
11.	Body Roll Rate	Deg/s	0.003906	Right Wing Down
12.	Body Yaw Rate	Deg/s	0.003906	Nose Right
13.	Body Long Acc'n	G	0.000122	Forward
14.	Body Lat Acc'n	G	0.000122	Right
15.	Body Normal Acc'n	G	0.000122	Up
16.	Inertial Vertical Acc'n	G	0.000122	Up

TABLE 2.4

SPECIFICATIONS FOR IRS ACCELEROMETERS AND GYROSCOPES

A-4 Accelerometers:

Scale Factor Repeatability	0.005% (1 - sigma, 1 year)
Scale Factor Nonlinearity	10 µg / g2 (1 - sigma)
Bias Repeatability	50 µg (1 - sigma, 1 year)
Bias Short Term Stability	5 µg (1 - sigma)
Maximum Acceleration	25 g

LG-8028B Gyros:

Scale Factor Repeatability	0.0005% (1 - sigma)
Bias Repeatability	0.01 deg / hr (1 - sigma)
Random Drift	0.003 deg / $\sqrt{hr}$ (1 - sigma)
Maximum Rate	400 deg / s

TABLE 2.5

SPECIFICATIONS FOR DOPPLER VELOCITY AND LORAN-C

Decca Doppler Radar Type 72:

VEL COMPONENT	UNITS	ACCURACY	RESOLUTION	POSITIVE SENSE
Longitudinal (U)	M/s	1.0	0.00781	Forward
Lateral (V)	M/s	1.0	0.00391	Right
Normal (W)	M/s	1.0	0.00195	Down

ARNAV R-40 Loran-C Receiver:

COMPONENT	UNITS	ACCURACY	RESOLUTION	POSITIVE SENSE
Latitude	Deg	0.00333	0.000167	North
Longitude	Deg	0.00471	0.000167	West

TABLE 2.6

NAE INERTIAL INSTRUMENTATION PACKAGE

INSTRUMENT	OUTPUT[1] TYPE	DESCRIPTION
Sperry C-12 gyro compass	S	Magnetic heading sensor
Kearfott T2109 vertical gyro	S	Pitch, roll attitude
Systron-Donner 4211 accels	A	Body axis accelerations (3)
Smiths 402-RGA rate gyros	A	Body axis angular rates (3)

[1] A - Analog S - Synchro

TABLE 2.7

NAE INERTIAL INSTRUMENTATION PACKAGE SPECIFICATIONS

PARAMETER	UNITS	RESOLUTION	RMS OF CALIBRATION
Compass Heading, C-12	Deg (Mag)	2.197×10^{-2}	8.565×10^{-2}
Pitch Attitude, Vertical Gyro	Deg	2.179×10^{-2}	3.669×10^{-1}
Roll Attitude, Vertical Gyro	Deg	2.276×10^{-2}	2.650×10^{-2}
Longitudinal Accel	M/s^2	3.048×10^{-3}	4.194×10^{-3}
Lateral Accel	M/s^2	3.058×10^{-3}	9.665×10^{-3}
Vertical Accel	M/s^2	9.572×10^{-3}	1.534×10^{-1}
Pitch Rate	Deg/s	5.600×10^{-3}	3.533×10^{-2}
Roll Rate	Deg/s	1.054×10^{-2}	5.410×10^{-2}
Yaw Rate	Deg/s	5.426×10^{-3}	4.066×10^{-2}

3.0 PRESENT TECHNIQUES FOR WIND COMPUTATION

3.1 Background

The measurement of atmospheric motion (winds and gusts) by an aircraft involves the calculation of the vector difference between the air motion relative to the aircraft and the aircraft's inertial velocity relative to the ground. The air vector is measured by the noseboom (Fig.1) and the associated pressure and temperature sensors which determine true airspeed and the angles of attack and sideslip. Since 1980, the inertial velocity sensing system onboard the Twin Otter has been based on a complementary filtering technique in which high frequency components are measured by an NAE package of accelerometers and rate/attitude gyros, and low frequency motions are sensed by a 3-axis Doppler radar velocity sensor (see Section 2 for details, also Ref. 4). This system has worked well, with an accuracy of better than 1.0 mps RMS, but can be degraded during flight in precipitation, when the Doppler radar locks onto the falling precipitation particles rather than the ground.

In 1987, the Litton LTN-90-100 IRS was acquired, initially to provide a second inertial velocity measurement, with plans for it to replace the Doppler-based system if it proved accurate and trouble-free. It was first used operationally on the Twin Otter in the October, 1987 segment of the First International Satellite Land Surface Climatology Field Experiment (FIFE - see Ref. 5). Since that time, the Litton IRS has been providing a second set of recorded inertial velocity data, and two new sets of wind measurements for comparison purposes.

3.2 Wind Computation Methods

The three different wind computation methods currently available onboard the Twin Otter are described below:

1) **Original Doppler/Inertial Winds (DI):** This is the calculation that has been used since 1980. The three orthogonal components of the wind are computed in aircraft axes using the true airspeed (TAS) vector from the noseboom and inertial velocities computed using a complementary filter method. Inputs to this complementary filter come from the NAE inertial instrumentation package plus the 3-axis Doppler radar. Once computed, the winds are resolved into earth-fixed axes using heading/attitude data from the magnetic compass and the attitude gyro.

2) **Litton Winds (L):** The inertial velocity components used in this computation are the direct outputs of the Litton IRS in earth-fixed axes. Consequently, the vector difference to derive the winds is performed in earth axes after the TAS vector undergoes an axis transformation using the Litton-measured heading and attitude angles.

3) **Doppler/Litton Winds (DL):** As with the DI winds, this computation is performed in aircraft axes using complementary filtering for the inertial velocity components. In this case, however, the accelerometer and rate gyro data come from the Litton IRS rather than from the NAE package, and the Litton heading and attitude angles are used to resolve the computed wind components into earth-fixed axes.

3.3   Wind Measurements and the Inertial Reference System (IRS)

During the Canadian 1988 Eulerian Model Evaluation Field Study (EMEFS), in which the NAE Twin Otter participated (Ref. 6), the Twin Otter instrumentation computed and recorded the three wind estimates listed above (i.e. DI, L and DL). EMEFS was the first project in which the Litton IRS was used for all flights, so it provided a good opportunity to compare the different wind derivation methods. The principal observation from this analysis (complete details can be found in Ref. 6) was that the Litton winds were less consistent than those computed using the other two methods. Variations in amplitude of 2 to 3 mps were routinely observed in the Litton winds, and the period of these variations was the so-called Schuler period of 84 minutes. These Schuler oscillation errors are caused by offset errors in the IRS accelerometers and gyros, and by initial misalignment errors, with the resulting inertial velocity error build-up governed by a well-known set of error dynamics equations (see Ref. 7 for details). The error levels observed were always just within the specifications quoted by the IRS manufacturer. This is disappointing, for errors in wind measurements of this magnitude are unacceptable; the original Doppler/Inertial system used in the Twin Otter can usually measure winds to an accuracy of 1 mps, except when operating in heavy precipitation.

One standard technique used to evaluate aircraft wind measuring systems is to fly a wind box. This is a square pattern, with sides of at least a one-minute duration, flown at an altitude where winds are expected to be steady with little or no turbulence. Comparison of winds averaged over the legs on reciprocal headings can be used to indicate the existence of an error in the true airspeed (TAS) or Doppler ground speed or both. This test cannot distinguish between a TAS and a ground speed bias error, though -- timed runs over a known ground track can be used for that purpose. Furthermore, Litton winds that are consistent around a wind box can lead to the false conclusion that they are accurate. Clearly, in view of the susceptibility of the IRS to Schuler oscillation errors, Litton winds can be consistent over the period of time required for a wind box, but still be inaccurate. On the other hand, consistency of Doppler winds (either DI or DL) around a wind box usually means that they are accurate.

Based on the results of several wind boxes flown during the 1988 EMEFS (see Ref. 6 for details), the following specific observations can be made:

1) The average Doppler/Inertial and Doppler/Litton winds for each box are very nearly equal. This is because both methods use complementary filtering, with the Doppler providing the low-frequency (mean) components. Any differences between these two methods are a result of higher frequency excursions from the different accelerometer and rate gyro signals used in the calculations. Different attitude angle and heading sources are used in the two methods as well (see Subsection 3.2).

2) The wind box-averaged Litton winds, when compared with the others, show discrepancies that correlate in direction and magnitude with the Schuler-induced IRS velocity errors.

3) The Litton winds show a consistency around the wind box (as measured by the standard deviations of wind direction and speed) close to that of the Doppler (DI and DL) winds. However, although they appear consistent, they are obviously inaccurate in cases where the Schuler velocity error is significant.

Table 3.1 effectively demonstrates the problem with Litton winds by comparing box-averaged winds for two EMEFS boxes flown in the same air mass at the same altitude only ten minutes apart. The mean Doppler/Inertial and Doppler/Litton winds for each box are nearly identical; however, the average Litton winds differ by 11 degrees and 3.5 mps because of the change in the Schuler velocity error in the short period of time from one wind box to the next.

All of the above comments on the drift of the Litton IRS apply to only the horizontal velocity components. Drifts in the vertical velocity component are removed in the IRS software using a continuous barometric altitude measurement passed to the IRS from the onboard microprocessor. The vertical wind component, derived using the vertical inertial velocity directly from the IRS, appears to have satisfactory accuracy.

Because of the accuracy degradation of the Doppler radar in precipitation and its generally noisy nature, the long range plan for the Twin Otter has been to replace the Doppler radar with the IRS, thereby saving weight and electrical power. The evaluation conducted during the 1988 EMEFS concluded that this is not yet possible **if one is using standard wind computation techniques**. The best overall winds for accuracy and consistency during EMEFS were the Doppler/Litton winds. The traditional Doppler/Inertial winds were only slightly less accurate, and the straight Litton winds were **not** acceptable.

TABLE 3.1

WIND BOX AVERAGES - DIRECTION (DEG TR) / SPEED (MPS)

	HDG	DOPPLER/ INERTIAL (DI)	LITTON(L)	DOPPLER/ LITTON (DL)
Wind Box #1:	NW	327/9.2	323/12.3	319/9.6
	SW	323/11.5	326/11.6	318/10.6
	SE	311/11.2	332/11.5	315/10.4
	NE	315/9.3	333/11.2	318/9.8
Mean Value -		**319/10.3**	**329/11.7**	**318/10.1**
Stnd Dev (Dir/Spd) -		**(006/1.06)**	**(004/0.41)**	**(002/0.41)**
Wind Box #2:	NW	322/9.4	334/8.9	320/9.4
	SW	320/10.2	337/7.4	316/9.8
	SE	313/10.7	344/8.1	315/10.1
	NE	314/9.2	346/8.4	319/9.7
Mean Value -		**317/9.9**	**340/8.2**	**318/9.8**
Stnd Dev (Dir/Spd) -		**(004/0.61)**	**(005/0.54)**	**(002/0.25)**

4.0   A KALMAN FILTER TECHNIQUE FOR ACCURATE VELOCITY SENSING

Because of the problem with accurate inertial velocity sensing from the LTN-90-100 IRS (as documented in Subsection 3.3), a Kalman filter-based integrated navigation algorithm has been developed in order to improve both position and velocity sensing onboard the Twin Otter. This section will discuss some of the details of the Kalman filter design.

4.1   The Linear Discrete-Time Kalman Filter

The linear, discrete-time version of the Kalman filter algorithm (Refs. 8, 9) assumes a physical system with an equivalent n^{th}-order, discrete-time dynamic model (derived from the original continuous-time model) of the form

$$x(k+1) = \Phi(k,k+1)\ x(k)\ +\ G(k)\ u(k) \tag{1}$$

where $x(k)$ is the nth-order system state vector evaluated at discrete time t_k; $\Phi(k,k+1)$ is the nxn state transition matrix over the time interval $t_k \rightarrow t_{k+1}$; $G(k)$ is the nxr plant noise gain matrix at t_k; and $u(k)$ is the rth-order vector of zero-mean, white, Gaussian (ZMWG) discrete plant noise processes having covariance matrix $Q(k)$ at t_k.

For the above dynamic system, let a discrete-time, m^{th}-order measurement process exist in the form

$$z(k+1) = H(k+1)\ x(k+1)\ +\ v(k+1) \tag{2}$$

where $z(k+1)$ is the measurement vector at time t_{k+1}, $H(k+1)$ is the mxn observation matrix and $v(k+1)$ is the mth-order measurement noise vector having covariance matrix $R(k+1)$ at t_{k+1}. Assume that noise vectors u and v are statistically independent (i.e. the components of u are uncorrelated with the components of v); and assume also that $x(0)$ is independent of both u and v. Define the following vector and matrix variables:

$x'(k+1)$, $P'(k+1)$ –   time update of the state vector and its covariance at t_{k+1} (i.e. just prior to a measurement update at time t_{k+1}).

$x(k+1)$, $P(k+1)$ –   optimal state estimate and its associated covariance at t_{k+1} (i.e. just after a measurement update at time t_{k+1}).

x_0, P_0 –   initial conditions on the state vector and its covariance (i.e. $x(0) = x_0$, $P(0) = P_0$).

Under the foregoing definitions and assumptions, it can be shown that the optimal estimate of the state vector at time t_{k+1} (i.e. $x(k+1)$), and its associated error covariance (i.e. $P(k+1)$), can be computed from the following set of five recursion equations that form the heart of linear, discrete-time Kalman filtering:

$x'(k+1)$	$=$	$\Phi(k,k+1)\ x(k)$	state time update
$P'(k+1)$	$=$	$\Phi(k,k+1)\ P(k)\ \Phi^T(k,k+1) + G(k)\ Q(k)\ G^T(k)$	error covariance time update
$K(k+1)$	$=$	$P'(k+1)\ H(k+1)\ [H(k+1)\ P'(k+1)\ H^T(k+1) + R(k+1)]^{-1}$	Kalman gain
$x(k+1)$	$=$	$x'(k+1) + K(k+1)\ [z(k+1) - H(k+1)\ x'(k+1)]$	state measurement update
$P(k+1)$	$=$	$P'(k+1) - K(k+1)\ H(k+1)\ P'(k+1)$	error covariance measurement update $\qquad\qquad$ (3)

with initialization of this recursive procedure provided by a priori knowledge of x_0 and P_0.

4.2 Software for Performing Discrete-Time Kalman Filtering

Numerically efficient, robust software exists for executing the foregoing set of five recursion equations, especially if certain simplifying assumptions can be made. There is a set of four relatively short FORTRAN 77 subroutines that perform the above vector/matrix calculations in a very efficient fashion. They are based on Bierman's UDU^T factorization algorithms (Ref. 10), which are generally acknowledged to be the most numerically stable, computationally efficient ones to use, especially for real-time applications. In order to avoid the matrix inversion that would normally be required in the Kalman gain equation (i.e. the third one of Eqns. 3), the assumption is made that the elements of z, the measurement vector, are statistically independent of each other (this is usually a valid assumption in practice). Under this assumption, the covariance matrix R is diagonal and the measurement vector z can then be processed in a one-at-a-time fashion. In essence, the Kalman gain vector/matrix equation is converted to a sequence of much simpler scalar/vector operations.

4.3 Integrated Navigation Using Kalman Filtering

Figure 2 shows a simplified block diagram representation of the Kalman filter integrated navigation configuration as it applies to the set of navigation sensors available on the NAE Twin Otter. In this so-called error state feedforward filter implementation (Ref. 11), the LTN-90-100 IRS is treated as a 'black box' deadreckoning system that outputs raw position, velocity and attitude data, corrupted with errors, at a sample rate of 16 Hz. Also shown is the barometric altimeter input to the IRS, required for its vertical channel baro-damping loop. Two additional navaids, an airborne Loran-C receiver and a Doppler velocity sensor, supply redundant navigational information that is used to form measurements that are processed by the Kalman filter algorithm. The differences in horizontal position (latitude and longitude components) between the IRS and the Loran-C receiver are used as one form of measurement. This particular measurement type can be processed by the Kalman filter as frequently as 1 Hz, the rate at which Loran-C data are acquired.

The second type of measurement data available for processing is derived from the Doppler strapdown (i.e. body axis) velocity components. As can be seen in Fig. 2, the Doppler U, V, and W velocity components are differenced with their IRS-derived counterparts, and these strapdown velocity differences are then processed by the Kalman filter. The data rate for the velocity difference measurements is the fundamental Doppler sample rate of 2 Hz. In this error state Kalman filter design, the dominant low frequency sources of error in the IRS, Loran-C receiver and the Doppler velocity sensor are statistically modelled; and these slowly varying errors are estimated in an on-line fashion based on the measurement data being processed in real time. The 16 Hz data stream of raw IRS data (position and velocity components) can then be corrected, in real time, using the error estimates generated by the Kalman filter. The Loran-C receiver and Doppler velocity sensor data can also be corrected for any significant low frequency errors detected by the filter. The basic update interval for the Kalman filter processing (i.e. the execution of Eqns. 3 for a new set of measurement data) is set at ten seconds -- more than adequate for 'tracking' the expected sources of error in the various navigation systems.

Important Features of the Error State Feedforward Approach-

It is worthwhile to list the important features of the error state feedforward approach to Kalman filter integrated navigation:

- By modelling the dynamics of the error states rather than the physical states of the system, the use of a _linear_ Kalman filter design is more likely to be a valid assumption.

- The error states and measurements used in the Kalman filter are all relatively small in magnitude, so numerical round-off error is usually not a problem even when cycling through the recursion equations (i.e. Eqns. 3) many times.

- The dominant error states of any navigation sensor vary slowly in time relative to the actual sample rate of the navigation data. Hence, discrete-time Kalman filtering can take place at a slow update rate but the error states so estimated can be applied to the navigation data at the much faster navigation data rate.

- With a discrete-time, linear Kalman filter design, efficient "off-the-shelf" FORTRAN software, such as Bierman's UDU^T factorization algorithms described in Subsection 4.2, can be used (Ref. 10).

4.4   IRS/Doppler/Loran-C Kalman Filter Design

4.4.1 Error States Chosen

For the IRS/Doppler/Loran-C Kalman filter design, there are a total of 24 error states modelled (Refs. 12 & 13 show details of the error modelling). The error states are divided into two groups -- i) 10 system error states that relate to the basic baro-damped IRS (i.e. errors in inertial position, velocity, attitude components and vertical loop acceleration error); and ii) 14 first-order Markov error states that correspond to the slowly varying, bias-like errors assumed to exist in the inertial sensors (i.e. bias errors in accelerometers, gyros, altimeter) and redundant navaids (i.e. Loran-C position component offsets, Doppler scale factor and boresight errors, sea currents). Table 4.1 lists all of the system error states, together with typical RMS values that would be used for the initial conditions, P_0, when running the Kalman filter. Table 4.2 is a list of the 14 Markov error states, again showing typical RMS initial condition values, as well as the nominal values of correlation times that would be assumed for the associated first-order Markov error processes. It should be noted that the last two error states in Table 4.2, the two sea bias components, would only be included in the Kalman filter in the case of an overwater flight.

TABLE 4.1

IRS SYSTEM ERROR STATES AND STATISTICS

	ERROR STATE	DESCRIPTION	INITIAL RMS VALUE	UNITS
1.	δL	Latitude Error	0.001667	Degrees
2.	$\delta \lambda$	Longitude Error	0.002357	Degrees
3.	δh	Altitude Error	10.0	Meters
4.	δv_N	North Velocity Error	0.10	M/sec
5.	δv_E	East Velocity Error	0.10	M/sec
6.	δv_z	Vertical Velocity Error	0.10	M/sec
7.	ε_N	N Axis Tilt Error	0.033333	Degrees
8.	ε_E	E Axis Tilt Error	0.033333	Degrees
9.	ε_z	Vertical Axis Tilt Error	0.100000	Degrees
10.	δa	Baro Loop Accel Correction	0.08	M/sec^2

TABLE 4.2

MARKOV ERROR STATES AND STATISTICS

	ERROR STATE	DESCRIPTION	INITIAL RMS VALUE	UNITS	CORRELATION TIME
11.	$B_{\omega x}$	X Axis Gyro Bias	0.02	Deg/hr	7500 s
12.	$B_{\omega y}$	Y Axis Gyro Bias	0.02	Deg/hr	7500 s
13.	$B_{\omega z}$	Z Axis Gyro Bias	0.02	Deg/hr	7500 s
14.	B_{ax}	X Axis Accel Bias	0.0006	M/sec^2	15,000 s
15.	B_{ay}	Y Axis Accel Bias	0.0006	M/sec^2	15,000 s
16.	B_{az}	Z Axis Accel Bias	0.0006	M/sec^2	15,000 s
17.	B_{hb}	Baro Altimeter Bias	60	Meters	5,000 s
18.	B_{LAT}	Loran Latitude Bias	0.00333	Degrees	15,000 s
19.	B_{LNG}	Loran Longitude Bias	0.00471	Degrees	15,000 s
20.	SF_U	Doppler Scale Factor	2 %	----	15,000 s
21.	B_V	Doppler V Boresight	2.30	Degrees	15,000 s
22.	B_W	Doppler W Boresight	1.15	Degrees	15,000 s
23.	SB_N	North Sea Bias	1.50	M/sec	900 s
24.	SB_E	East Sea Bias	1.50	M/sec	900 s

4.4.2 Plant Dynamics (Φ, G, Q)

The full 24 x 24 discrete state transition matrix Φ for the Kalman filter design is derived from the continous-time version of the error state equations, the details of which can be found in Ref. 14. The general relationship between the continous-time matrices, F(t) and G(t), and their discrete-equivalent counterparts, Φ (k, k + 1) and G(k) can be expressed as follows:

$$\Phi_{i,j}(k,k+1) = \int_{t_k}^{t_{k+1}} F_{i,j}(t)\, dt; \quad i,j = 1\ldots\ldots 24; \quad i \neq j$$

$$\Phi_{i,i}(k, k+1) = 1 + \int_{t_k}^{t_{k+1}} F_{i,i}(t)\, dt; \quad i = 1\ldots\ldots 10$$

$$\Phi_{i,i}(k,k+1) = e^{-\Delta T/t_i}; \quad i = 11\ldots\ldots 24$$

$$G_{i,j}(k) = \frac{1}{\Delta T} \int_{t_k}^{t_{k+1}} G_{i,j}(t)\, dt; \quad i,j = 1\ldots\ldots 24; \tag{4}$$

where $\Delta T = t_{k+1} - t_k$ is a constant equal to ten seconds, the t_i's are the Markov error state correlation times and the integrations are performed numerically using a simple trapezoidal integration algorithm.

A list of the first ten discrete-equivalent ZMWG noise components (i.e. elements of $u(k)$) included in the Kalman filter design is shown in Table 4.3 along with typical values for the associated standard deviations. Note that these components correspond to integrated random noise effects over the Kalman filter update interval (i.e. ΔT) of ten seconds. The rest of the noise components are discrete-equivalent versions of the so-called Markov plant noises associated with error states # 11 --> # 24 in Table 4.2. Their standard deviations are determined from the filter update interval (ΔT), correlation time and initial RMS level of the associated Markov error state. For simplicity in the filter design, all plant noise components are assumed to have constant variances that are not affected by aircraft manoeuvring. This results in a Q matrix that is diagonal and has all components constant with time.

TABLE 4.3

PLANT NOISE COMPONENTS AND STATISTICS

COMPONENT		DESCRIPTION	RMS VALUE	UNITS
1.	$u_{\omega x}$	X Gyro Random Drift	2.3×10^{-6}	Deg
2.	$u_{\omega y}$	Y Gyro Random Drift	2.3×10^{-6}	Deg
3.	$u_{\omega z}$	Z Gyro Random Drift	2.3×10^{-6}	Deg
4.	u_{ax}	X Accel Random Noise	3.0×10^{-4}	M/s
5.	u_{ay}	Y Accel Random Noise	3.0×10^{-4}	M/s
6.	u_{az}	Z Accel Random Noise	3.0×10^{-4}	M/s
7.	u_{gN}	North Random Gravity	3.0×10^{-4}	M/s
8.	u_{gE}	East Random Gravity	3.0×10^{-4}	M/s
9.	u_{gz}	Vertical Random Gravity	3.0×10^{-4}	M/s
10.	u_{hb}	Altimeter Random Noise	9.64	M-s

11. --> 24. : Discrete Markov Plant Noise Components Corresponding To Markov Error States 11 --> 24

4.4.3 Measurement Process (H, R)

Recall that there are two types of measurements that are being processed by the Kalman filter: i) measurements based on Loran-C position data, and ii) measurements based on Doppler velocity data.

Measurements Based on Loran-C -

These measurements, taken at discrete times t_{k+1}, will consist of the two simultaneous, independent difference quantities, $z_1(k+1)$ and $z_2(k+1)$, where

$$z_1(k+1) = LAT_{INS}(t_{k+1}) - LAT_{LOR}(t_{k+1})$$

$$z_2(k+1) = LNG_{INS}(t_{k+1}) - LNG_{LOR}(t_{k+1}) \tag{5}$$

The 24-element rows of the **H** matrix that are associated with these two measurements (i.e. the first two rows of **H**) are given very simply as:

$$H_1 = (1\ 0\ 0\ 0 \ldots \ldots -1\ 0\ 0\ 0\ 0\ 0\ 0)$$

$$H_2 = (0\ 1\ 0\ 0 \ldots \ldots 0\ -1\ 0\ 0\ 0\ 0\ 0) \tag{6}$$

The noise variances assumed for these two measurements, r_1 and r_2, are the first two diagonal elements of the overall measurement noise covariance matrix **R**. Nominal values of $r_1 = (0.07\ \text{arc min})^2$ and $r_2 = (0.1\ \text{arc min})^2$ are assigned to these parameters, based on the observed performance of the Loran-C receiver onboard the NAE Twin Otter. The Loran-based measurement data is available at a 1 Hz rate; but the normal Kalman filter measurement update rate is only 0.1 Hz (i.e. every ten seconds).

Measurements Based on Doppler Radar -

Recall that the fundamental measurements produced by the Doppler velocity sensor are the body axis velocity components U_D, V_D, W_D, (forward, to the right and down being the positive senses in the body axis coordinate frame). It is then necessary to process velocity differences between the IRS and the Doppler system in this body axis frame. In order to do this properly, the IRS velocity components must be transformed into equivalent body axis components and, as well, the Doppler velocity components must be corrected for lever arm effects. The lever arm effects are due to the fact that the location of the Doppler radar antenna is not coincident with the location of the IRS.

Let C_G^b be the transformation matrix that converts IRS velocity data in geographic coordinates (i.e. v_N, v_E, v_z) into equivalent components in body axis coordinates (i.e. U_I, V_I, W_I). This transformation matrix is re-computed continuously in the Kalman filter, based on the Euler angle (i.e. attitude) data available from the LTN-90 IRS, using the following equations:

$$
\begin{aligned}
C_{1,1} &= \cos\theta\ \cos\psi \\
C_{1,2} &= \cos\theta\ \sin\psi \\
C_{1,3} &= \sin\theta \\
C_{2,1} &= \sin\theta\ \sin\phi\ \cos\psi - \cos\phi\ \sin\psi \\
C_{2,2} &= \sin\theta\ \sin\phi\ \sin\psi + \cos\phi\ \cos\psi \\
C_{2,3} &= -\cos\theta\ \sin\phi \\
C_{3,1} &= \sin\theta\ \cos\phi\ \cos\psi + \sin\phi\ \sin\psi \\
C_{3,2} &= \sin\theta\ \cos\phi\ \sin\psi - \sin\phi\ \cos\psi \\
C_{3,3} &= -\cos\theta\ \cos\phi
\end{aligned}
\tag{7}
$$

The IRS velocity components, converted into body axis coordinates, can then be computed as:

$$
\begin{aligned}
U_I &= C_{1,1}\ v_N + C_{1,2}\ v_E + C_{1,3}\ v_z \\
V_I &= C_{2,1}\ v_N + C_{2,2}\ v_E + C_{2,3}\ v_z \\
W_I &= C_{3,1}\ v_N + C_{3,2}\ v_E + C_{3,3}\ v_z
\end{aligned}
\tag{8}
$$

In order to look at lever arm effects, define l_{DI} as the lever arm position vector from the Doppler radar antenna to the LTN-90 IRS. This position vector is measured in body axis coordinates and has components l_x, l_y, and l_z. Define ω_B as the angular body rate vector of the IRS, expressed in body axis coordinates. It is directly available from the LTN-90 dataport and has components ω_{Bx}, ω_{By}, ω_{Bz}. Corrected Doppler velocity components (i.e. U_{DC}, V_{DC}, W_{DC}) are then calculated as:

$$U_{DC} = U_D - \omega_{Bz} l_y + \omega_{By} l_z$$

$$V_{DC} = V_D + \omega_{Bz} l_x - \omega_{Bx} l_z$$

$$W_{DC} = W_D - \omega_{By} l_x + \omega_{Bx} l_y \tag{9}$$

The three Doppler-based measurement components available at discrete times t_{k+1} can then be written as

$$z_3(k+1) = U_I(k+1) - U_{DC}(k+1)$$

$$z_4(k+1) = V_I(k+1) - V_{DC}(k+1)$$

$$z_5(k+1) = W_I(k+1) - W_{DC}(k+1) \tag{10}$$

The 24-element rows of H that are associated with these three measurements (i.e. rows 3, 4 and 5) have the following non-zero elements:

$$H_3: \quad h_{3,4}, \quad h_{3,5}, \quad h_{3,6}, \quad h_{3,20}, \quad h_{3,23}, \quad h_{3,24}$$

$$H_4: \quad h_{4,4}, \quad h_{4,5}, \quad h_{4,6}, \quad h_{4,21}, \quad h_{4,23}, \quad h_{4,24}$$

$$H_5: \quad h_{5,4}, \quad h_{5,5}, \quad h_{5,6}, \quad h_{5,22} \tag{11}$$

and details of their calculation can be found in Ref. 14. The noise variances assumed for these three measurements, r_3, r_4 and r_5, consist of diagonal elements 3, 4 and 5 of the 5 x 5 measurement noise covariance matrix R. Nominal values chosen for these variances are $r_3 = (1.63\text{m/s})^2$, $r_4 = (3.26\text{m/s})^2$ and $r_5 = (1.63 \text{ m/s})^2$, based on an analysis of typical Doppler radar data from the Twin Otter. Doppler-based measurements are available at a 2 Hz rate, much faster than the basic Kalman filter update rate of 0.1 Hz.

As stated before, by assuming that measurement components $z_1 \rightarrow z_5$ are statistically independent, the measurements and their associated statistics (i.e. z_i and H_i, r_i) can be processed in a one-at-a-time fashion using the software algorithms mentioned in Subsection 4.2.

5.0 KALMAN FILTER RESULTS USING FLIGHT TEST DATA

The Kalman filter computer code was initially verified using simulated Twin Otter navigation data, in a very controlled fashion, so that the 'true' aircraft trajectory was always known. Analysis of filter runs using this simulated data confirmed that the Kalman filter design was sound and that its predicted accuracy specifications were being met. Of much more interest was the Kalman filter performance using 'real world' data collected onboard the Twin Otter during typical operational flights. To this end, two sets of specialized flight test data (each about 1.5 hours in duration) have been collected. During these particular flights, a route was chosen such that the aircraft overflew selected visual landmarks whose positions were known to an accuracy of better than 0.1 nm. This allowed for an assessment of navigational accuracy over the entire flight. As well, a wind box and/or railroad runs on reciprocal headings were conducted as part of each flight in order to evaluate wind computation accuracy. Figure 3 shows a track plot for the second of these flights - the numbers from 1 --> 15 correspond to the locations of the visual landmarks along the route. The first flight followed a trajectory identical to the one shown in Fig. 3, except that the wind box was omitted.

5.1 Accuracy of Filter-Based Position/Velocity Sensing

Figure 4 is a series of plots depicting the buildup in IRS positional error (both latitude and longitude components) during the course of the flights, as determined by position comparisons at the visual landmark locations. Positional error drift rates of about 1 nm/hour are typical for this quality of IRS, together with a Schuler-induced oscillating error (with an 84 minute period) of perhaps 1 nm peak-to-peak. In contrast, Fig. 5 shows a similar series of plots for the Loran-C position errors during the same flights. Note the bounded nature of these errors, with both position error components consistently below 0.2 nm in magnitude. The small, bounded nature of Loran-C errors makes airborne Loran-C an ideal redundant navaid to use, in a Kalman filter integrated navigation scheme, to identify the dominant IRS errors. Figures 6a and 6b show time series plots of the three Doppler-based measurements (i.e. U, V and W velocity differences) for each of the flights. As can be seen, the velocity measurements are quite noisy due to the large level of so-called fluctuation noise in the Doppler velocity components (1.5 mps RMS for each of U and W, 3.0 mps RMS for V). Compared to airborne Loran-C, Doppler velocity data (from our particular Doppler radar sensor) is less than ideal as a source of Kalman filter measurements.

Due to the noisy, variable nature of the Doppler data, the best Kalman filter results occur when Loran-C is the sole source of measurement information. Figure 7 shows filter estimates of IRS horizontal position error during the two flights, together with RMS bounds (dashed lines) computed by the filter to reflect the accuracy level of these error estimates. In all cases, the bounds are estimated to be approximately +/- 0.2 nm; and the actual accuracy of IRS position error estimation (as determined by the visual landmark locations) always falls within these bounds. This is a good indication of a robust Kalman filter design.

Of particular interest for wind computation is the Kalman filter accuracy when estimating IRS horizontal velocity errors. Figure 8 shows filter estimates of IRS horizontal velocity error components during the course of the two flights, along with RMS bounds (dashed lines) indicating the estimation accuracy level to be expected. The RMS bounds for the accuracy of velocity error estimation settle out at about +/- 0.3 mps, implying that IRS velocity error estimates from the Kalman filter are accurate to within +/- 0.3 mps in an RMS sense. Although we do not have an independent, accurate measure of inertial velocity to use in order to verify this estimation accuracy, it should be noted that the filter estimates of IRS velocity errors are very consistent when compared to the slope of the position error traces (which are known to be accurate to within +/- 0.2 nm). The plots in Fig. 8 include shaded areas to highlight the velocity error levels that occur during wind boxes or railroad runs. Due to the baro-damped vertical channel of the IRS, its vertical velocity error is already maintained within the +/- 0.3 mps limits, (Kalman filter analysis confirms this) and no additional improvement is possible via Kalman filtering.

The Kalman filter calculates estimates of the fundamental errors in the Doppler velocity sensor as well as those of the IRS itself (see Table 4.2). Figures 9a and 9b display time series plots of the filter-estimated Doppler errors for the data from each of the navigation flights. As can be seen, scale factor errors in the U channel can easily reach 1.5% --> 2%, even after careful calibration, and are quite variable because of the terrain sensitivity of this particular Doppler system. Similarly, the V channel boresight error is no. particularly constant, with variations that exceed 1 degree at times. With the 60 mps groundspeed typically attained by the Twin Otter, uncalibrated Doppler velocity errors in each of the U and V channels can reach 1 mps. The shaded areas in the plots of Figs. 9a and 9b indicate the time intervals for the railroad runs or wind box that were conducted during each flight. Note the significant levels (and the variability) of Doppler scale factor and V boresight error at that time -- this would certainly degrade the accuracy of wind computations for any Doppler-based complementary filter approach. Kalman filter analysis of typical Doppler error time histories clearly points out the fundamental limitations of using Doppler velocity data, in an inertial/Doppler complementary filter mix, for wind computation

5.2 A Comparison of Three Kalman Filter Configurations

The baro-damped LTN-90-100 IRS inertial data is critical to the IRS/Doppler/Loran-C Kalman filter design that is depicted in Fig. 2. However, there are three different measurement configurations that can be analyzed (based on different combinations of the redundant navaid data), each of which assumes that the essential IRS data is available. These three configurations are as follows: i) only Loran-C position

navaid measurements, ii) the combination of Loran-C and Doppler navaid measurements and iii) only Doppler velocity navaid measurements. Kalman filter IRS velocity error estimation results for all three filter configurations, and both sets of flight test data, are shown in Figs. 10 to 13. The case i) results (Loran only) are the most accurate, due to the high quality nature of the Loran-C measurement data. Next in accuracy would be the case ii) results (i.e. Loran-C/Doppler measurement combination) -- there is some accuracy degradation due to the inferior quality of the Doppler velocity data slightly corrupting the results, but the error traces are fundamentally the same as in case i). Also, in both of these cases the RMS error bounds settle out at about 0.3 mps for each component. Finally, the case iii) (Doppler only) results are the least accurate, as judged by the wider RMS bounds (+/- 0.7 mps on average) and sensitivity to aircraft manoeuvres. However, even in the Doppler-only measurement case, the dominant trends in the IRS velocity error traces of case i) are retained. A comparison of position error estimation for the three filter configurations (see Figs. 14 to 17) reveals that case i) and case ii) results are almost identical, with position errors consistently below 0.2 nm in magnitude, while case iii) (i.e. Doppler-only) results degrade to about 0.6 nm RMS, even under ideal Doppler conditions. It should be stressed that the Doppler-only results shown here are probably overly optimistic simply because of the special racetrack flight pattern and the number of turns involved in the flight trajectory. A more "benign" flight trajectory would result in poorer estimation of the Doppler sensor errors and, hence, reduced navigational accuracy from the Kalman filter. The foregoing comparisons serve to point out that, in the absence of Loran-C position data, there is still a significant improvement in inertial velocity (and positioning) accuracy to be gained from 'mixing' Doppler and IRS data using the more sophisticated Kalman filter approach, rather than the traditional complementary filter approach.

5.3 Wind Computation Using the Kalman Filter Approach

The final results to be discussed are based on run average wind data from the two special navigation flights that have been analyzed. Table 5.1 compares run average values for all four wind measurement methods, and for the various railroad runs and wind boxes that occur in each flight. The run average results for the Kalman filter winds (i.e. KL) are highlighted in the last column of Table 5.1, and should be considered the accurate 'reference winds' to be compared with those of the other three error-prone methods (i.e. DI, L and DL -- see Subsection 3.2).

In the case of Flight # 1, only reciprocal railroad runs were flown, each leg being just under 3 minutes in duration. For this flight, winds were moderate and reasonably steady, but there was a significant drop in wind speed at the end of the first leg of the railroad runs (this shows up clearly in the KL run averages). The results demonstrate the very significant errors that can occur in both the raw IRS-based winds (L) and the Doppler-based winds (DI and DL). The large errors in the L wind computations (as high as 1.7 mps, compared with KL) are a direct consequence of the large IRS errors in the north velocity component at that point in the flight (see Fig. 8). Similarly, the large errors in the DI and DL results (as high as 2 mps) are related to the existence of significant Doppler errors at that point in time. As a matter of fact, the variations in DI and DL errors, from one railroad run leg to the next, correlate nicely with the observed variations in the Doppler error states (as estimated by the Kalman filter -- see Fig. 9a).

For Flight # 2, reciprocal railroad runs (3 minutes per leg) and a wind box (1 minute per side) were flown just a few minutes apart (see track plot of Fig. 3). The winds were light and variable -- not ideal for checking out the consistency of the various wind measurement techniques. According to Table 5.1, there are more noticeable differences between the DI and DL Doppler-based wind techniques during Flight # 2, as compared to the Flight # 1 results. This is probably due to the existence of more high frequency information in the wind data (due to the gusty conditions during Flight # 2), and these components are being measured by a different set of inertial sensors for the DI winds as compared to the DL winds. Both the DI and DL results show significant errors (at times exceeding 1 mps), and a Kalman filter analysis of the Doppler error states confirms the error levels that are observed (see Fig. 9b). A comparison of L and KL results reveals very good agreement during both the railroad runs and the wind box. This is due to the fact that IRS velocity errors are quite small (about 0.2 mps on average -- see Fig. 8) during this part of the flight. If the wind box had occurred earlier in the flight, the results would have been different -- note, from Fig. 8., how IRS north velocity error builds up to almost 1 mps during the early stages of Flight # 2.

TABLE 5.1

RUN AVERAGES - DIRECTION (DEG TR) / SPEED (MPS)

	HDG	DI	L	DL	KL
Flight #1:	NE	349/7.5	351/9.3	352/7.5	352/7.6
(RR Runs)	SW	349/7.6	353/6.7	347/7.4	353/5.3
	NE	001/6.4	359/6.8	358/6.6	358/5.8
		---------	---------	---------	---------
Mean Value -		353/7.2	354/7.6	352/7.2	354/6.2
Stnd Dev (Dir/Spd) -		(005/0.55)	(003/1.20)	(005/0.40)	(003/0.99)
Flight #2:	NE	031/2.2	022/3.2	027/2.3	021/3.1
(RR Runs)	SW	032/2.4	058/2.4	029/2.1	059/2.2
	NE	058/1.9	044/2.3	047/1.9	041/1.9
		---------	---------	---------	---------
Mean Value -		040/2.2	041/2.6	034/2.1	040/2.4
Stnd Dev (Dir/Spd) -		(013/0.21)	(015/0.40)	(009/0.16)	(015/0.51)
Flight #2:	W	355/1.9	295/0.8	336/1.6	300/0.9
(WindBox)	S	333/3.4	330/1.6	327/2.7	325/1.7
	E	345/3.9	354/3.8	349/3.9	350/3.8
	N	009/3.0	354/3.0	004/3.4	349/3.1
		---------	---------	---------	---------
Mean Value -		350/3.1	333/2.3	344/2.9	331/2.4
Stnd Dev (Dir/Spd) -		(013/0.74)	(024/0.93)	(014/0.86)	(020/1.14)

6.0 CONCLUSIONS AND FUTURE WORK

6.1 Conclusions

1) With Loran-C measurements, the Kalman filter can consistently provide IRS-based velocity accuracy to a level of 0.3 mps RMS and horizontal positioning accuracy to a level of 0.2 nm RMS. Because the vertical channel of the IRS is baro-damped, vertical velocity accuracy is better than 0.3 mps RMS even without Kalman filtering, and no additional improvement is gained through filtering.

2) There is no further improvement in accuracy to be gained by processing Doppler measurements along with Loran-C measurements.

3) For Doppler-only measurements, IRS velocity accuracy is approximately 0.7 mps RMS. Position accuracy deteriorates to about 0.6 nm RMS, even under the best conditions for Doppler, due to the absence of an accurate, bounded source of positional information.

4) Based on 3), it is worthwhile retaining the Doppler system onboard the Twin Otter, as part of the Kalman filter configuration, for situations in which Loran-C coverage is not available. Alternatively, a GNS-500 VLF receiver (having virtually worldwide coverage) is available as a replacement for the Loran-C receiver, but with reduced accuracy.

5) This Kalman filter approach to airborne wind measurement ensures that the dominant source of error is no longer the sensing of inertial velocity but, rather, the measurement of the TAS vector. Any inconsistencies in wind data, based on wind boxes or intercomparisons, can then be attributed solely to the air data system and appropriate action taken.

6.2 Future Work

1) The Kalman filter algorithm will first be incorporated as a standard part of the Twin Otter playback program, allowing for improved wind computations during post-flight analysis.

2) A more powerful airborne microprocessor (a DEC MicroVax-II) is soon to be installed onboard the Twin Otter. Once that occurs, the Kalman filter software will be installed in it and employed for real-time wind computations.

3) If inconsistencies greater than 0.3 mps are still observed in wind box data, or intercomparison runs, a careful study will be conducted into other potential sources of error in the Twin Otter's wind measurement system.

4) At some point in the near future, the feasibility of installing a GPS receiver onboard the Twin Otter will be assessed with a view to gaining some experience with an IRS/GPS Kalman filter configuration. This sensor combination has the potential for producing 16 Hz inertial velocity data with a real-time absolute accuracy of 0.1 mps RMS in each of the three components.

7.0 ACKNOWLEDGEMENTS

8.0 REFERENCES

1. Technical Description of LTN-90-100 Inertial Reference System, Litton Aero Products, Canoga Park, Calif., May 1984.

2. Decca Overhaul Manual, Doppler Type 70 Series. The Decca Navigator Co., Ltd., Surrey, England, Sept. 1973.

3. R-40(AVA-1000A) Operation Manual. ARNAV Systems, Inc., Salem, Oregon, Feb. 1985.

4. MacPherson, J.I.
   Morgan, J.M.
   Lum, K.
   The NAE Twin Otter Atmospheric Research Aircraft. NAE Report LTR-FR-80, National Research Council of Canada, March 1981.

5. MacPherson, J.I.
   NAE Twin Otter Operations In FIFE. NAE Report LTR-FR-104, National Research Council of Canada, August 1988.

6. MacPherson, J.I.
   NAE Twin Otter Operations In The 1988 Eulerian Model Evaluation Field Study. NAE Report LTR-FR-107, National Research Council of Canada, April 1989.

7. Britting, K.R.
   Inertial Navigation Systems Analysis. John Wiley & Sons, Inc., Toronto, 1971.

8. Gelb, A.
   (editor)
   Applied Optimal Estimation. The M.I.T. Press, Cambridge, Massachusetts, 1974.

9. Leach, B.W.   An Introduction To Kalman Filtering. NAE Miscellaneous Report 57, National
                           Research Council of Canada, March 1984.

10. Bierman, G.J.   Factorization Methods For Discrete Sequential Estimation. Academic Press,
                           New York, 1977.

11. Maybeck, P.S.   Stochastic Models, Estimation, And Control Volume 1. Academic Press,
                           New York, 1979.

12. Widnall, W.S.   Inertial Navigation System Error Models.   Intermetrics Incorporated Report
    Grundy, P.A.   TR-03-73, Cambridge, Massachusetts, May 1973.

13. Leach, B.W.   Error State Feedback Kalman Filter Designs For An Airborne
                           Doppler/Heading System. NAE Report LTR-FR-100, National Research
                           Council of Canada, January 1987.

14. Leach, B.W.   A Kalman Filter Integrated Navigation Design For The NAE Twin Otter
                           Atmospheric Research Aircraft. NAE Report in progress.

PLASMA DISPLAY

2nd AIRSPEED, ALTITUDE

ROSEMOUNT 858
(α, β, AIRSPEED, ALTITUDE)

VIDEO CAMERAS

ATTITUDE GYRO

ROSEMOUNT TEMPERATURE PROBE

RADIO ALTIMETER

CONSOLE KEYBOARD NAVIGATION
SYSTEM CONTROLS

STREAMER RECORDER

ACCELEROMETERS, RATE GYROS

COMPUTER SYSTEM

LITTON 90 INERTIAL
REFERENCE SYSTEM

LORAN C ANTENNA

DECCA DOPPLER RADAR ANTENNA

DOPPLER RADAR
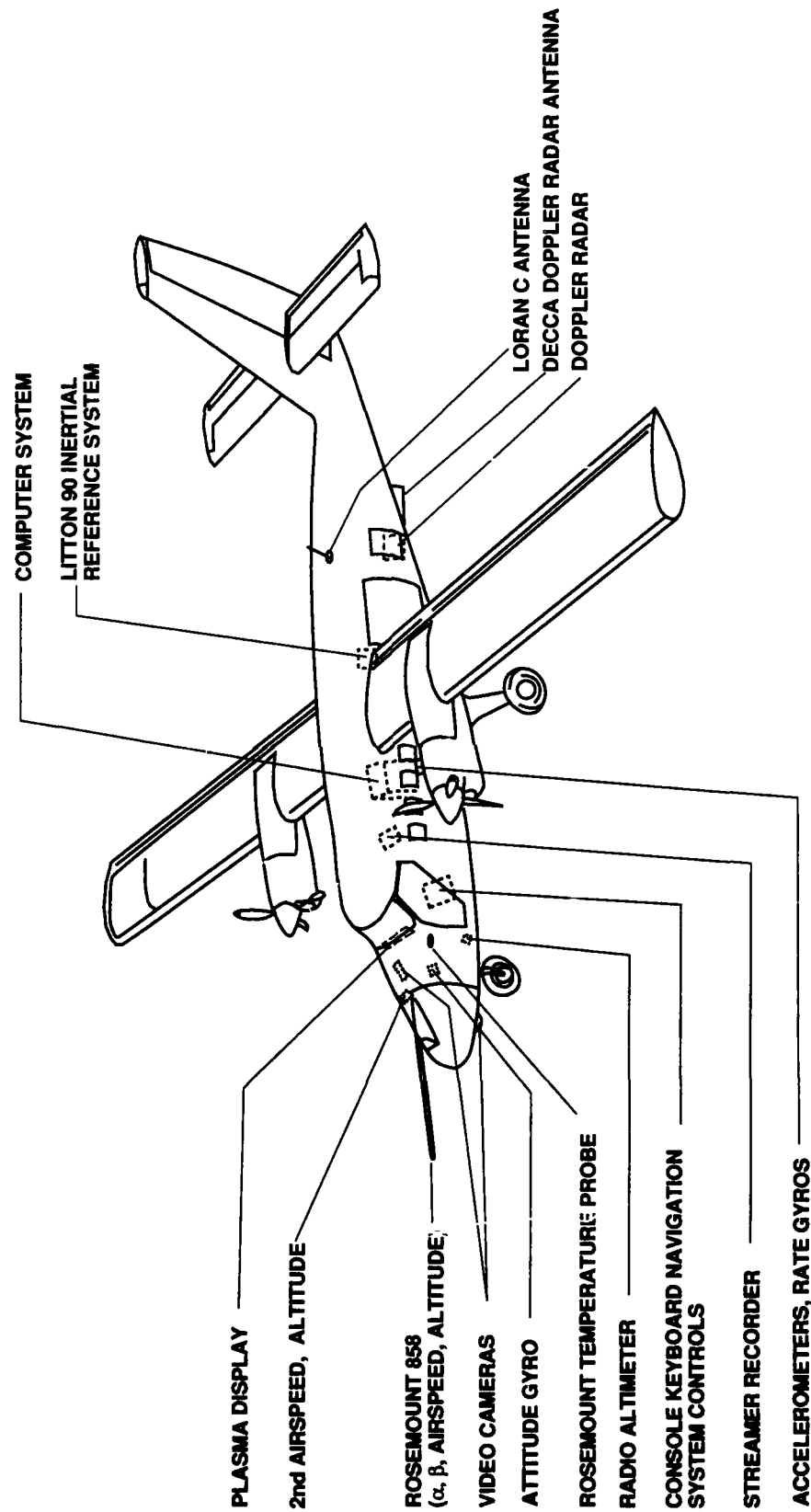
**FIG. 1: NAE TWIN OTTER ATMOSPHERIC RESEARCH AIRCRAFT AS
INSTRUMENTED FOR AIRBORNE WIND MEASUREMENT**

22
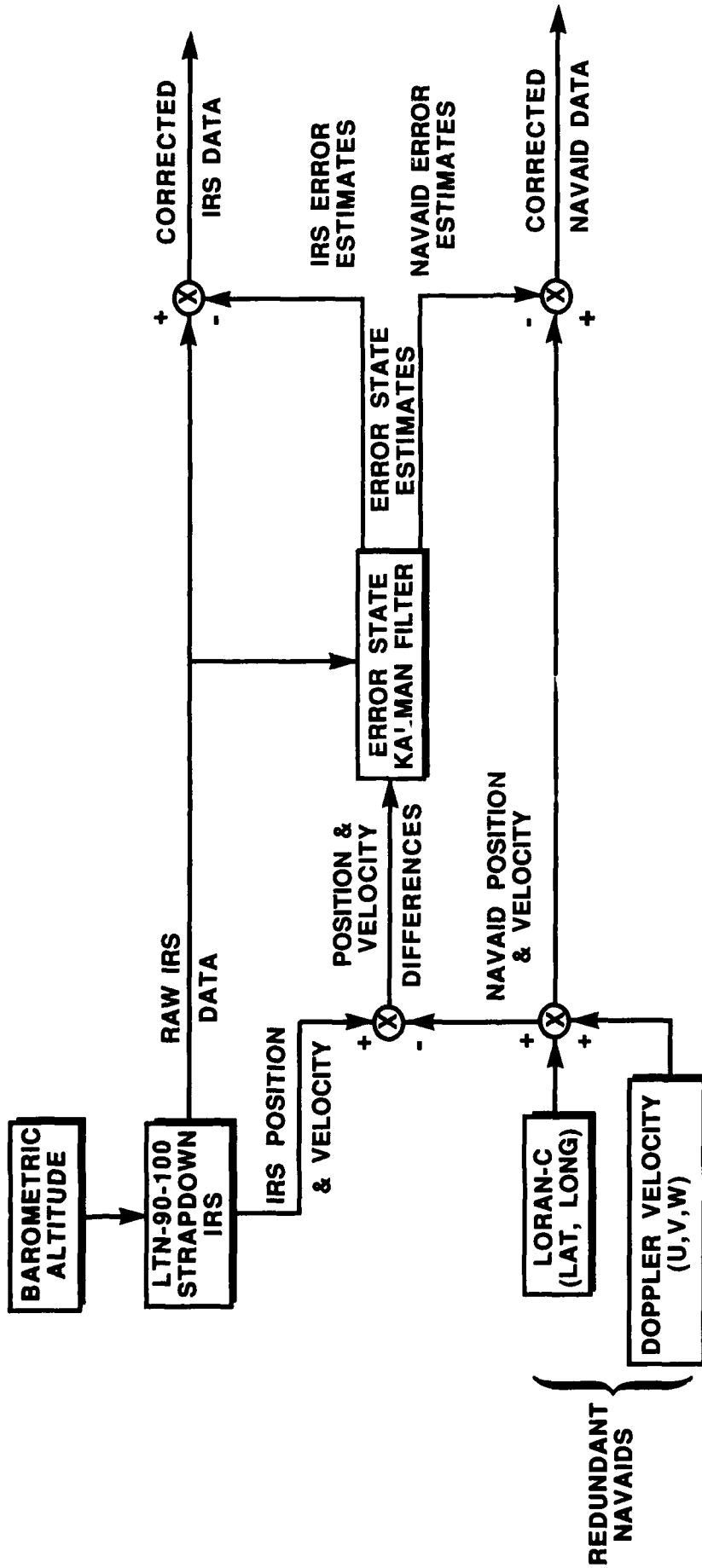
FIG. 2: IRS/DOPPLER/LORAN-C KALMAN FILTER CONFIGURATION
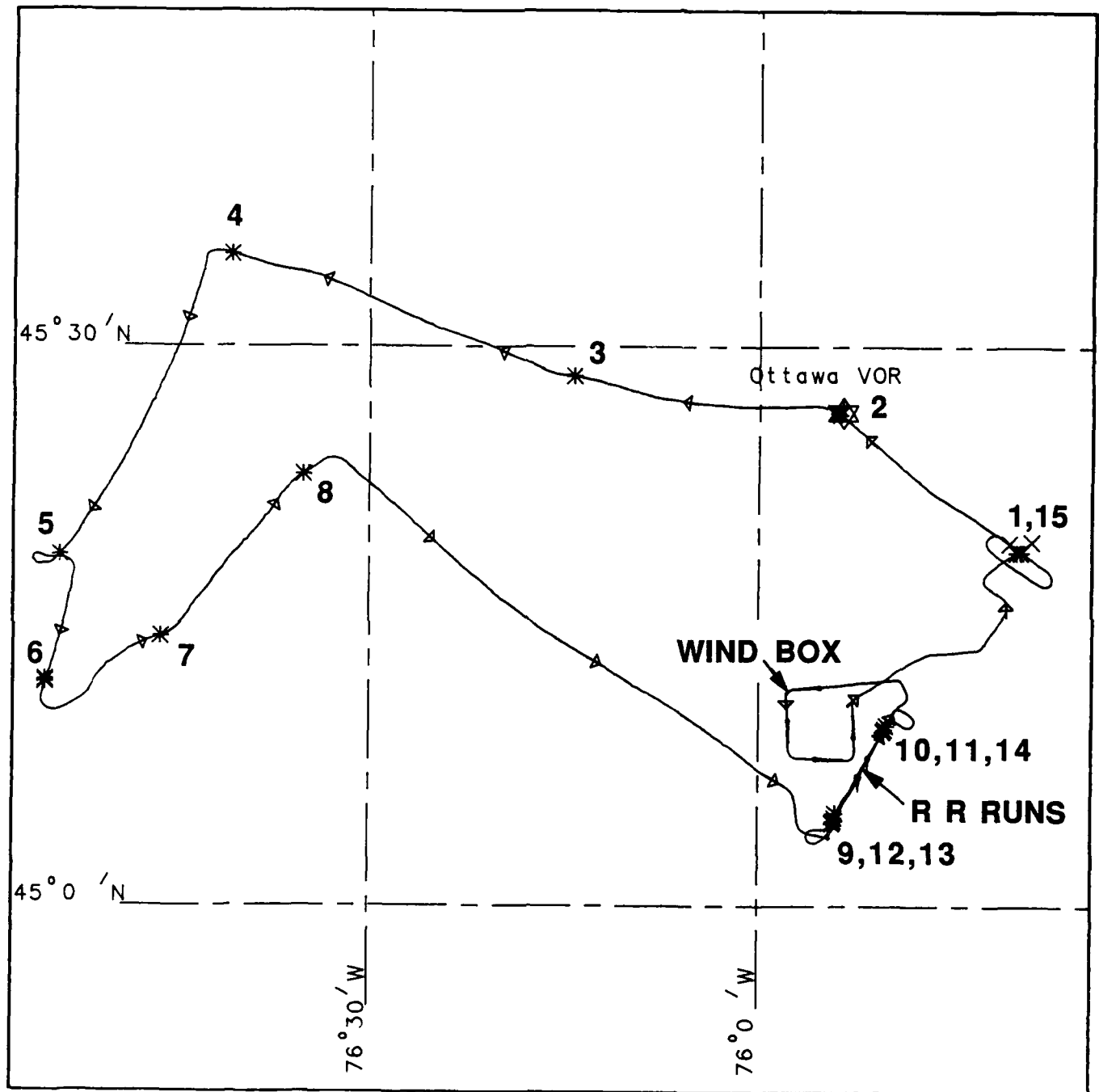
FIG. 3: TRACK PLOT FOR MAY 17/89 FLIGHT

24
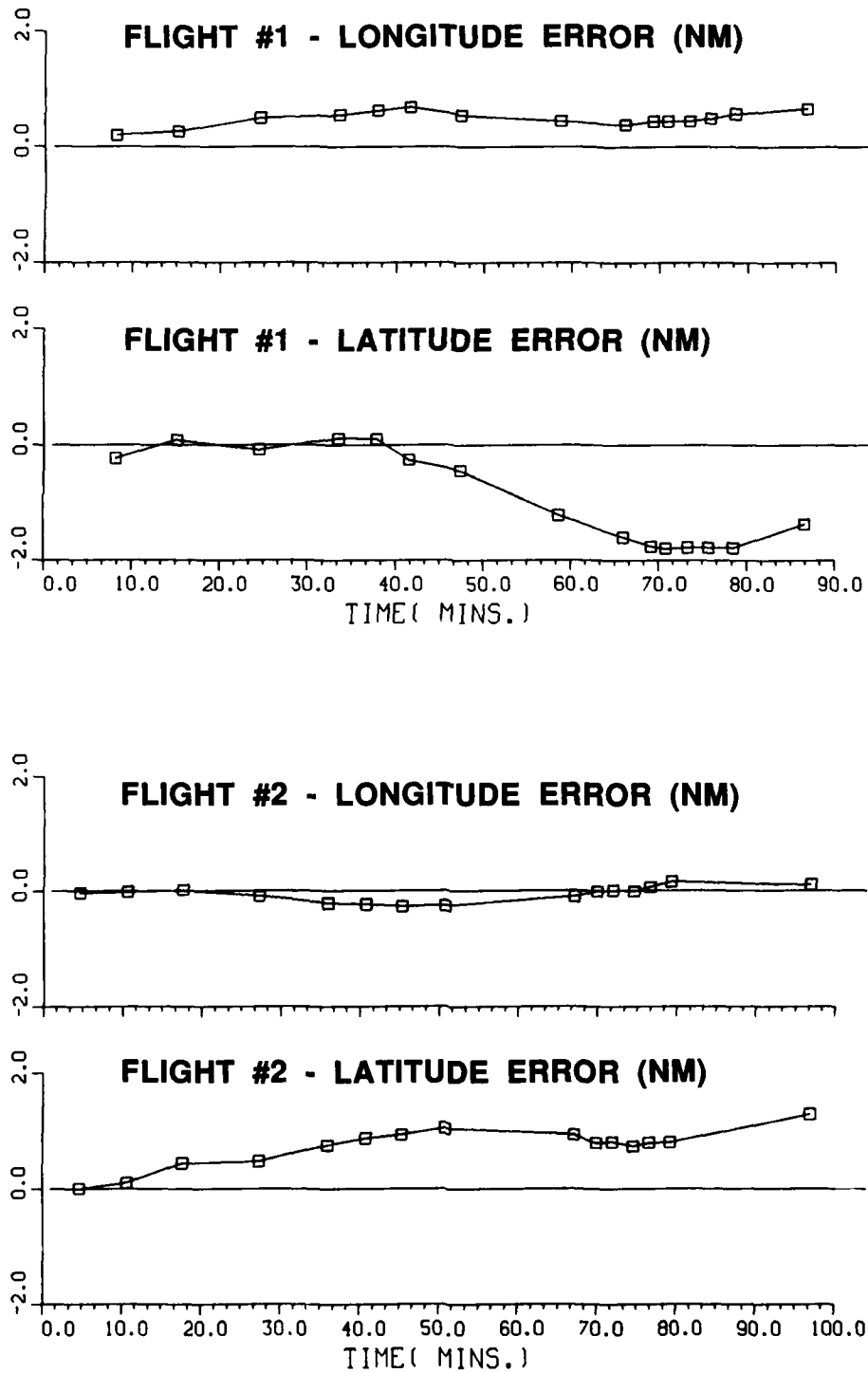
FIG. 4: IRS POSITION ERRORS
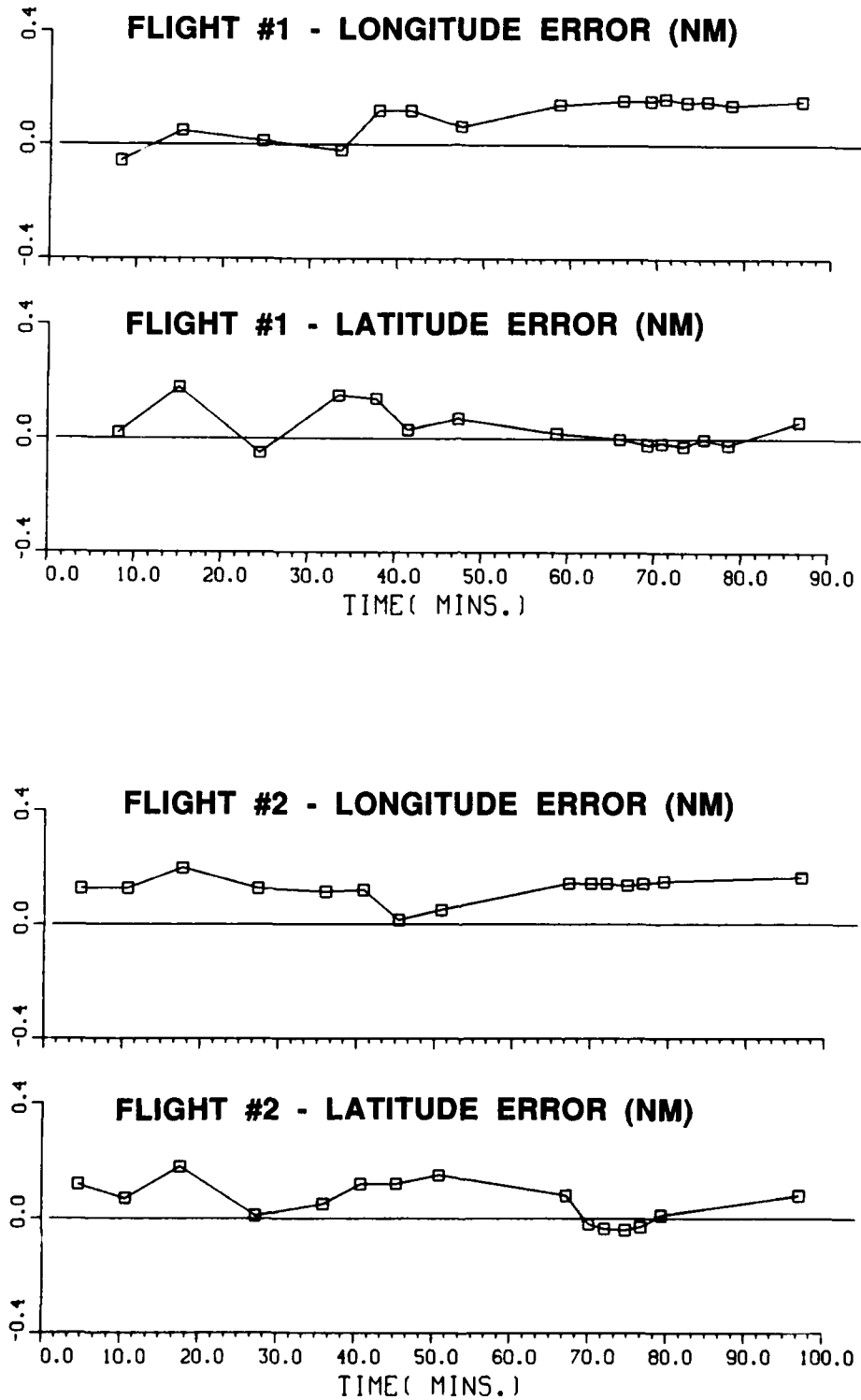
FIG. 5: LORAN-C POSITION ERRORS
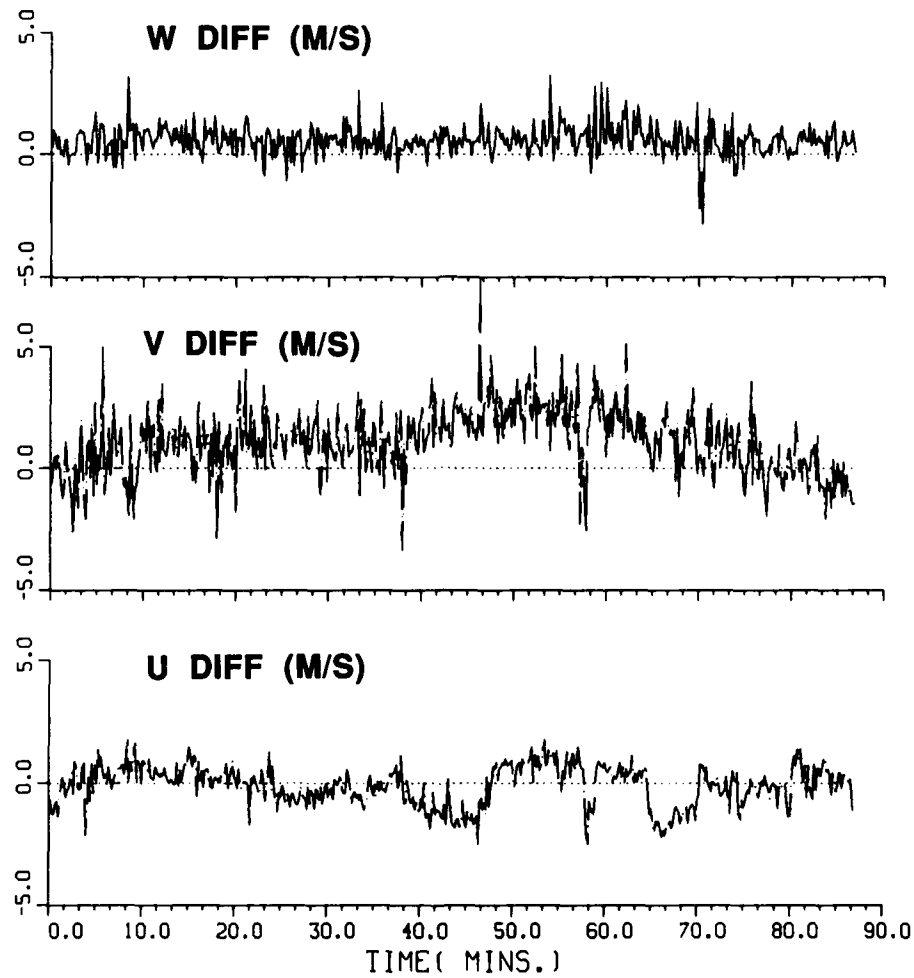
FLIGHT #1 DATA

FIG. 6a: DOPPLER VELOCITY MEASUREMENTS
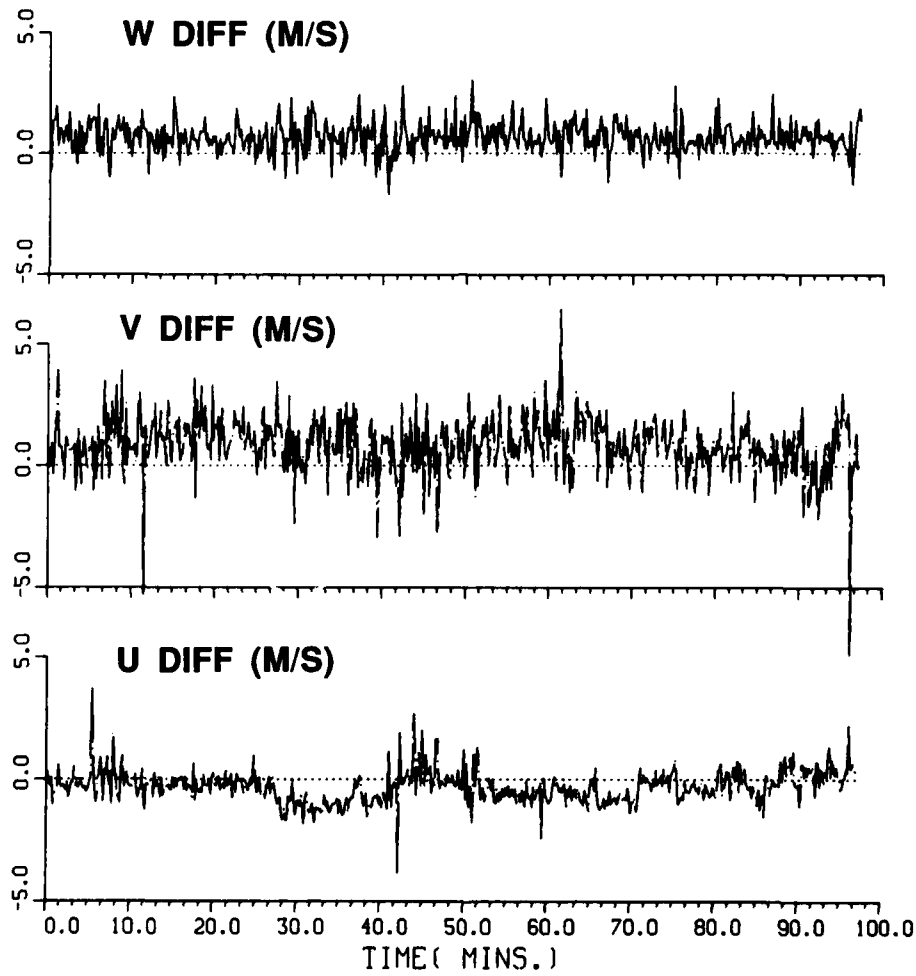
FLIGHT #2 DATA

FIG. 6b: DOPPLER VELOCITY MEASUREMENTS

28

FLIGHT #1 – LATITUDE ERROR (NM)

FLIGHT #1 – LONGITUDE ERROR (NM)

TIME (MINS.)

FLIGHT #2 – LATITUDE ERROR (NM)

FLIGHT #2 – LONGITUDE ERROR (NM)

TIME (MINS.)
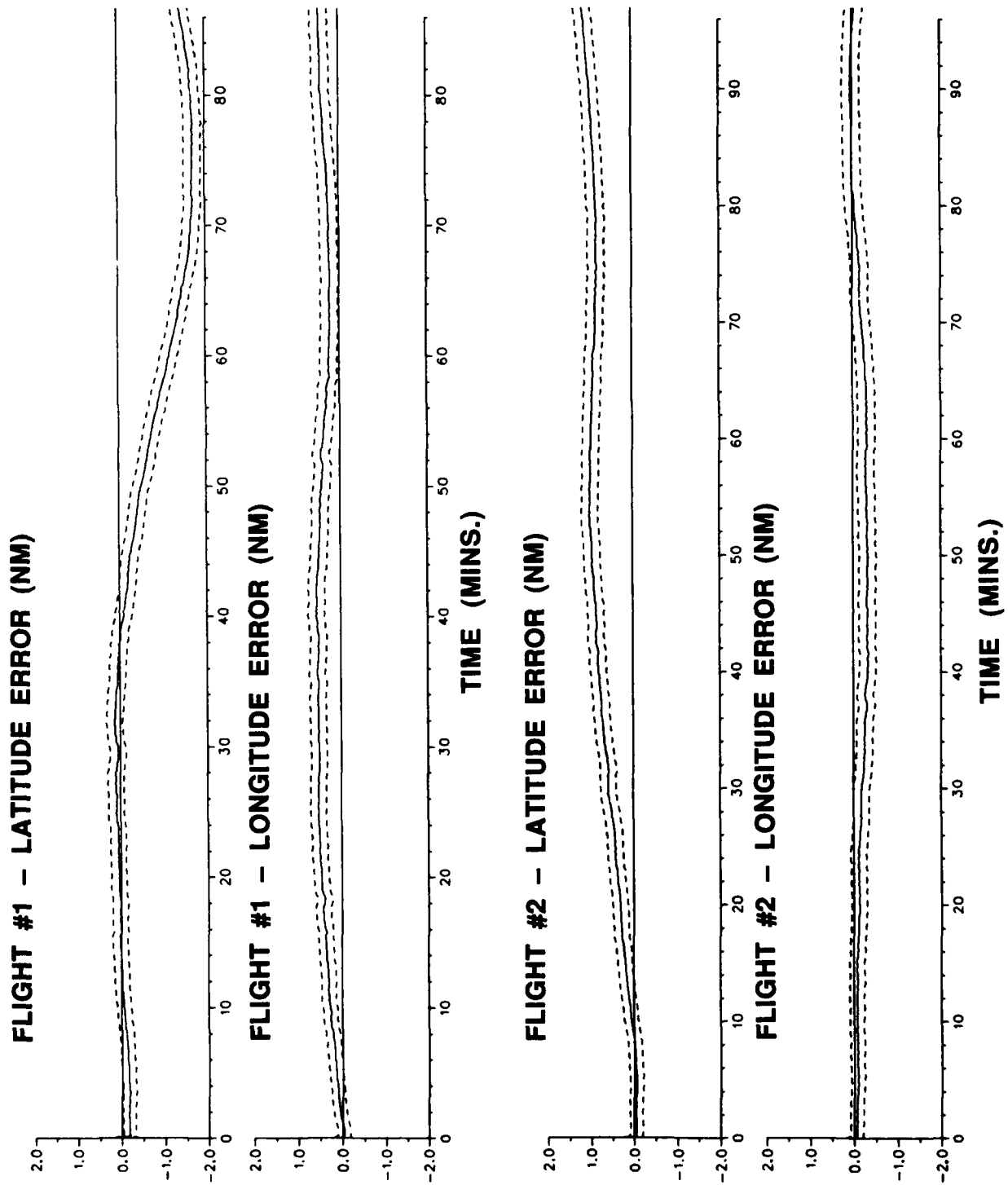
FIG. 7: KALMAN FILTER ESTIMATES OF IRS POSITION ERRORS

FLIGHT #1 - NORTH VELOCITY ERROR (M/S)

FLIGHT #1 - EAST VELOCITY ERROR (M/S)

FLIGHT #2 - NORTH VELOCITY ERROR (M/S)

FLIGHT #2 - EAST VELOCITY ERROR (M/S)
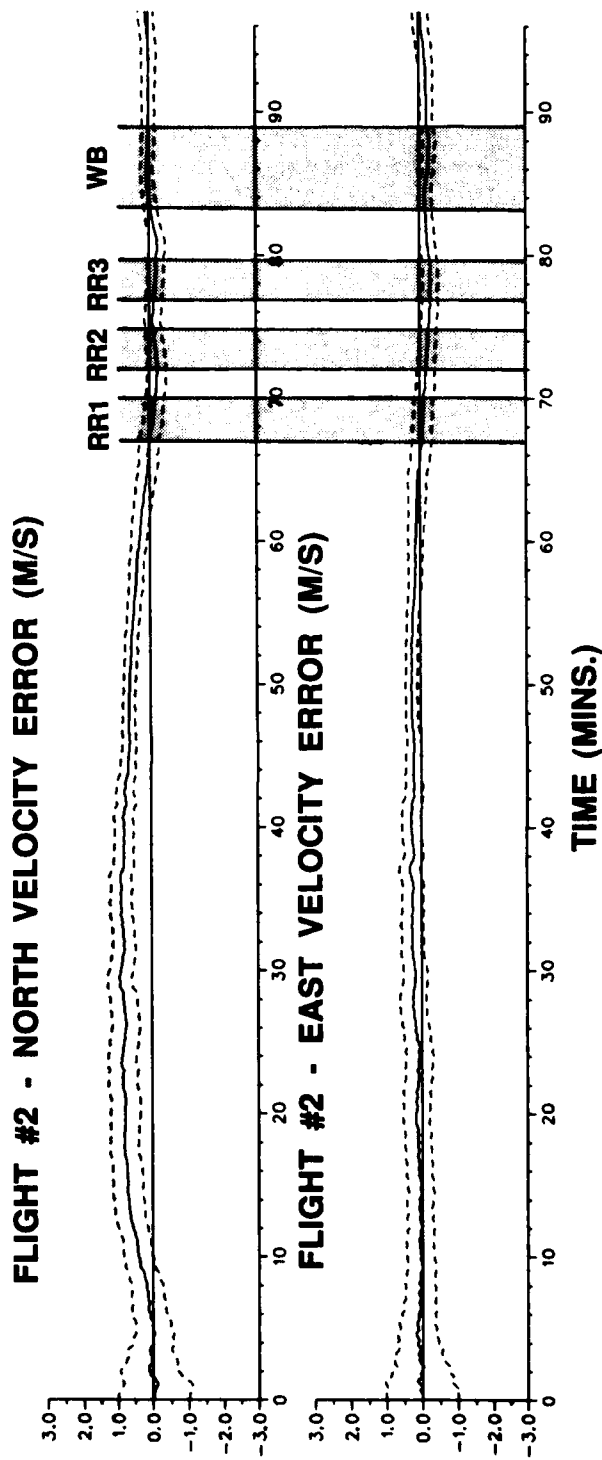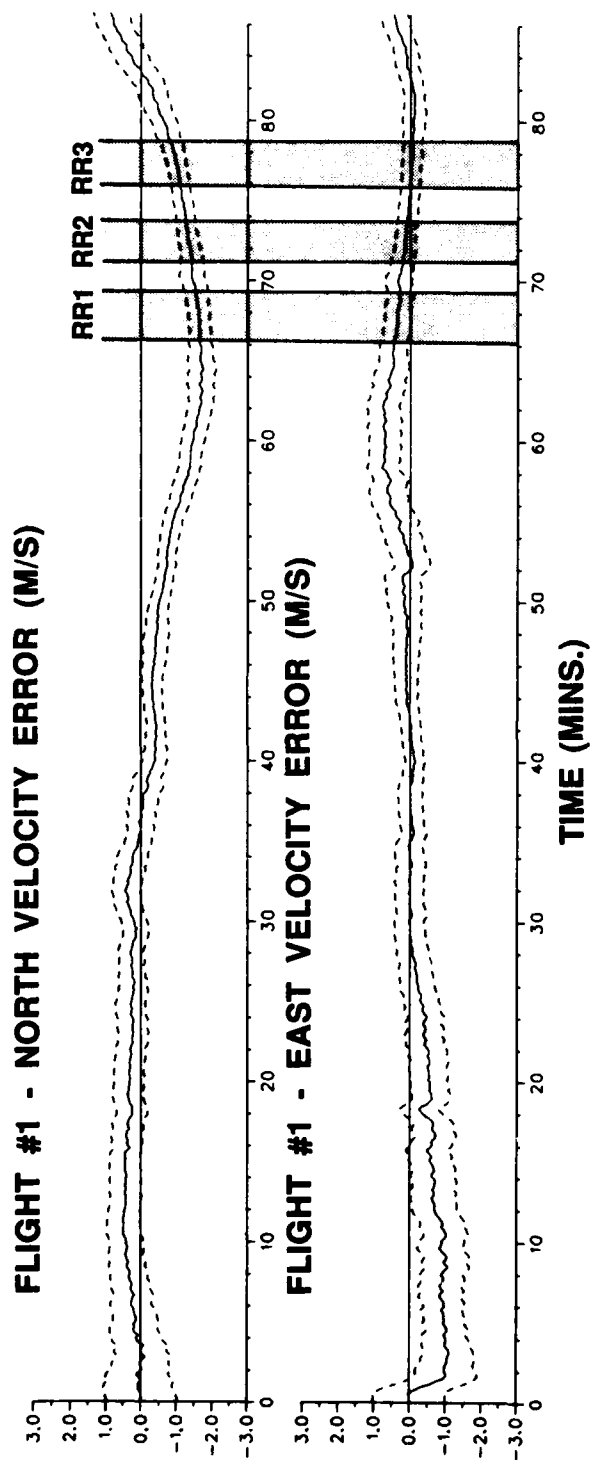
TIME (MINS.)

FIG. 8: KALMAN FILTER ESTIMATES OF IRS VELOCITY ERRORS

FIG. 9a: KALMAN FILTER ESTIMATES OF
DOPPLER VELOCITY ERRORS

FLIGHT #1 DATA

DOPPLER SCALE FACTOR ERROR

DOPPLER V BORESIGHT ERROR (DEG)

DOPPLER W BORESIGHT ERROR (DEG)
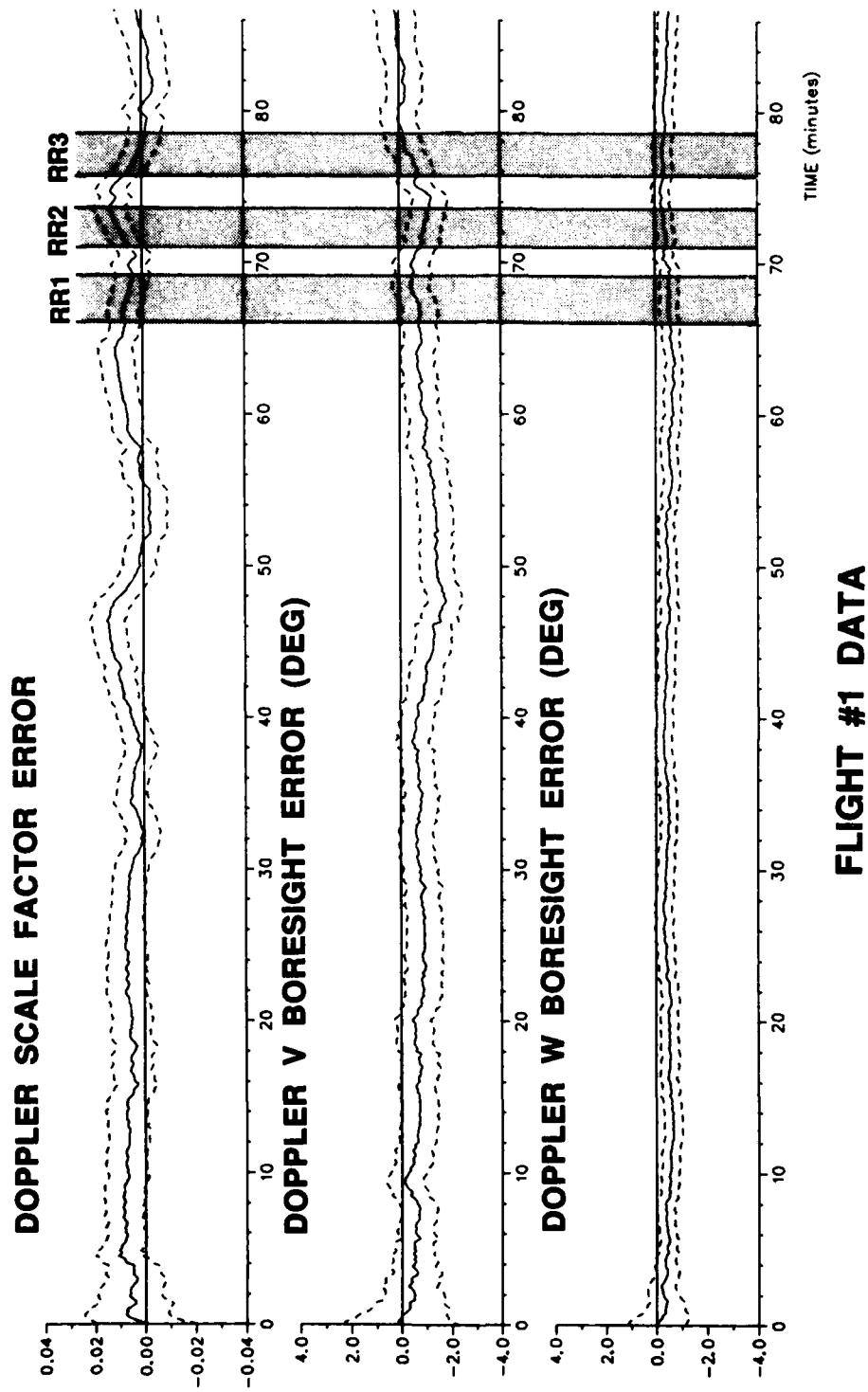
TIME (minutes)

FIG. 9b: KALMAN FILTER ESTIMATES OF
DOPPLER VELOCITY ERRORS

FLIGHT #2 DATA

NORTH VELOCITY ERROR (M/S) - LORAN KF

NORTH VELOCITY ERROR (M/S) - LORAN/DOPPLER KF
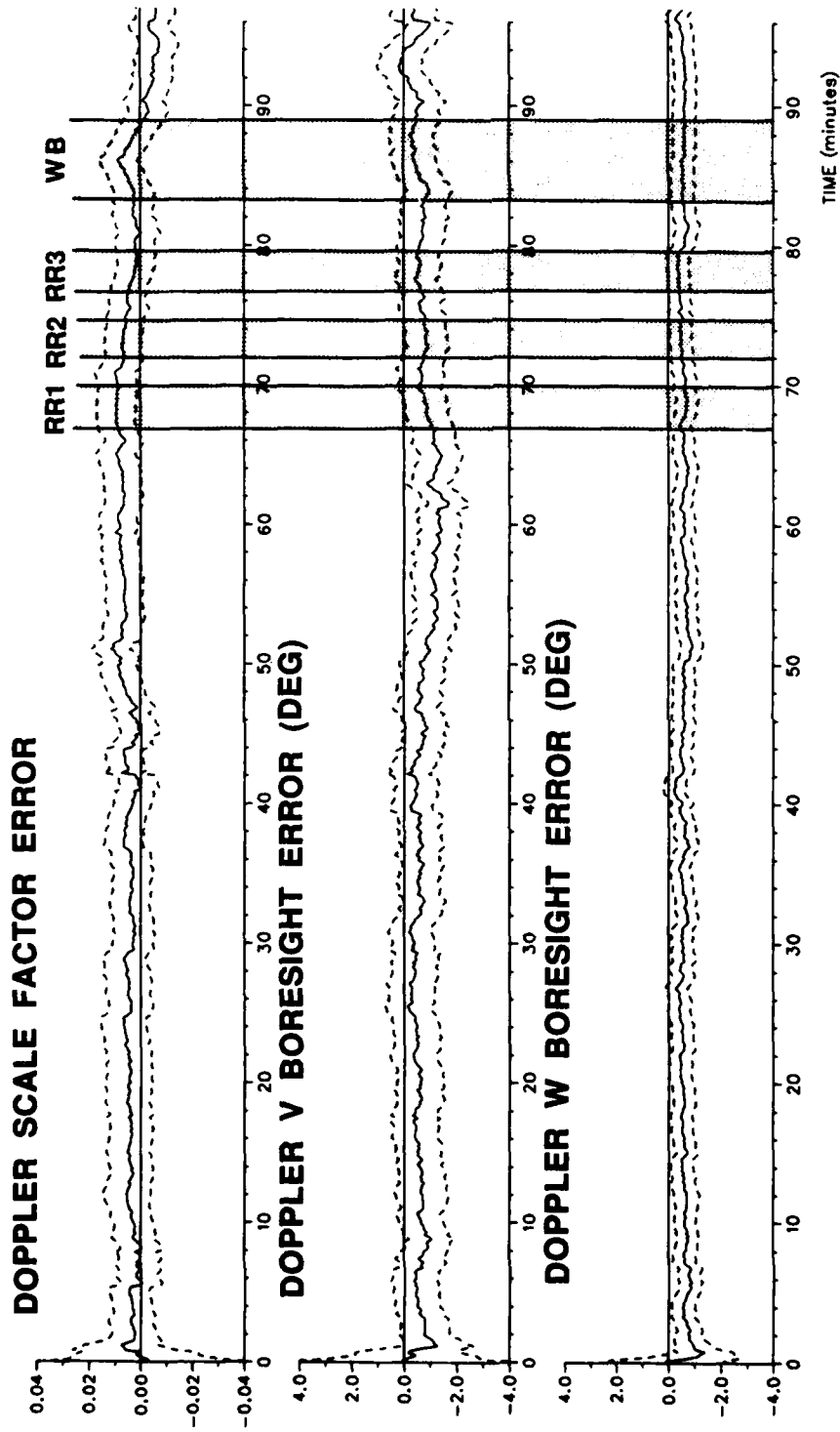
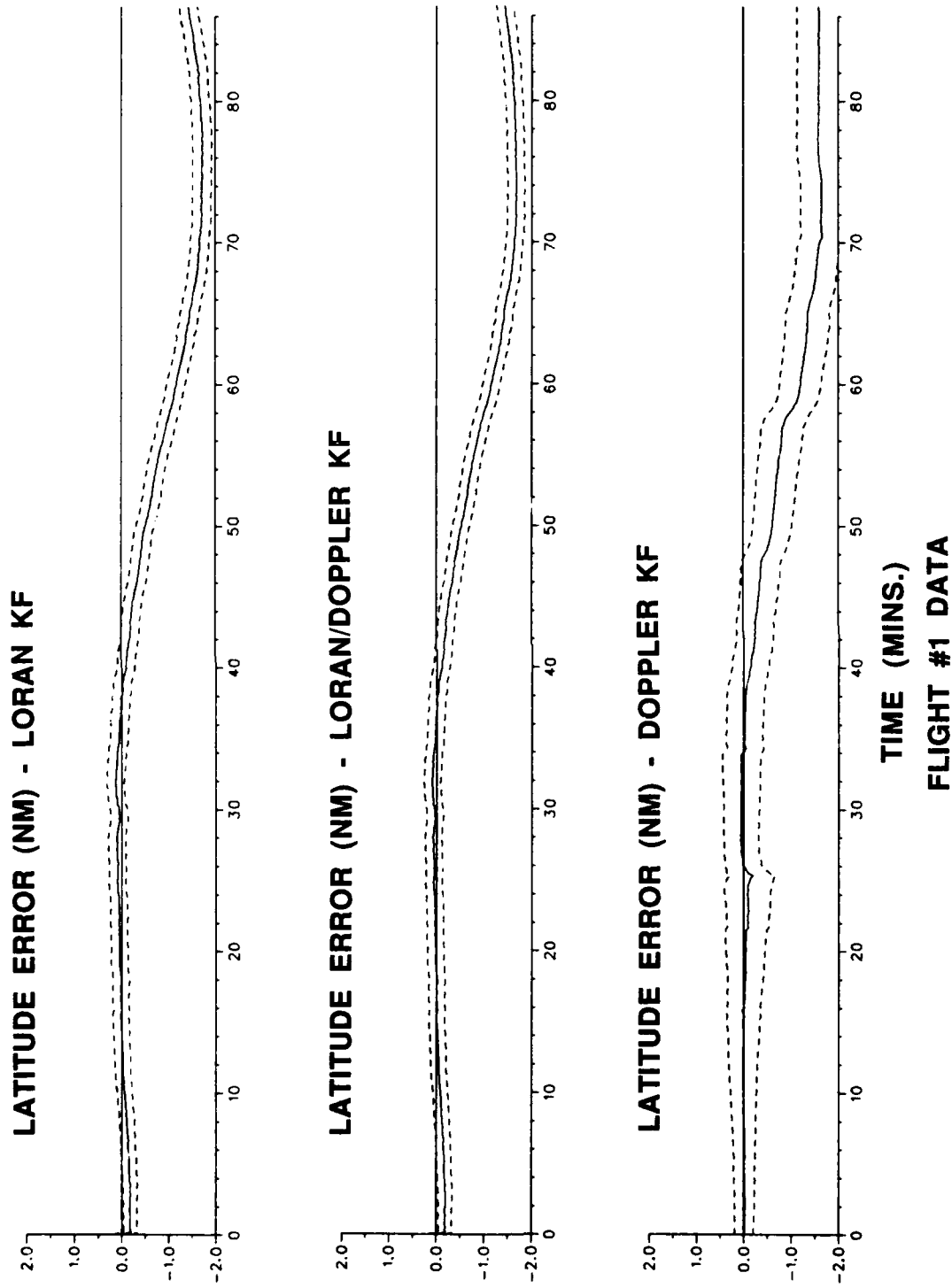NORTH VELOCITY ERROR (M/S) - DOPPLER KF
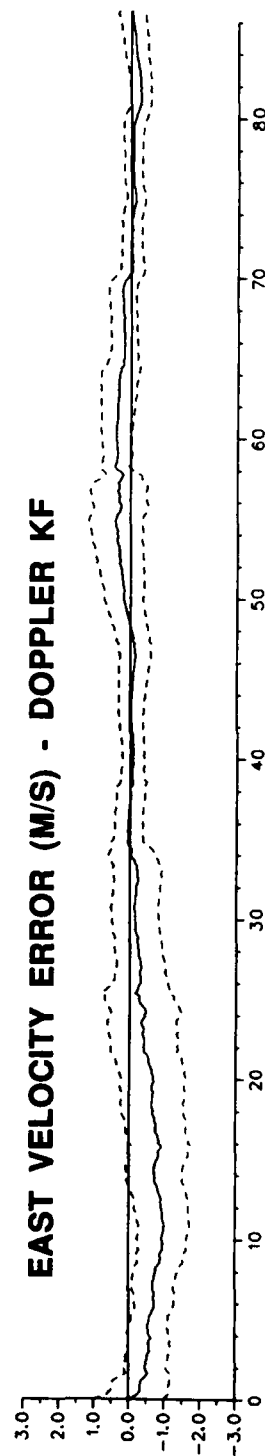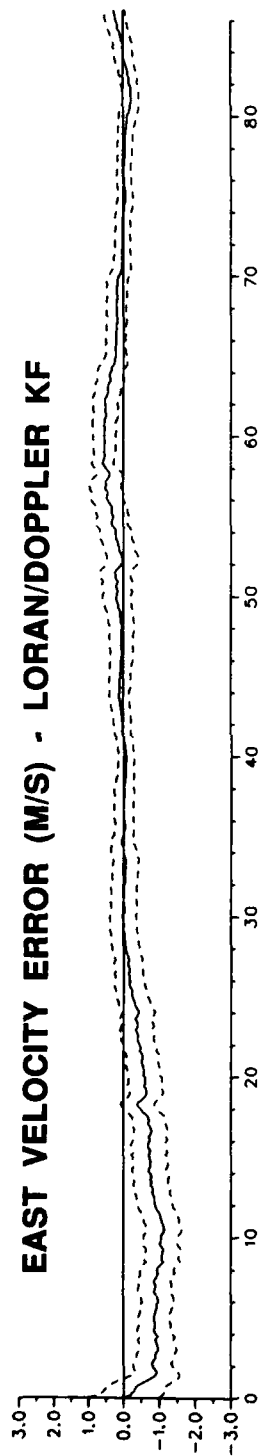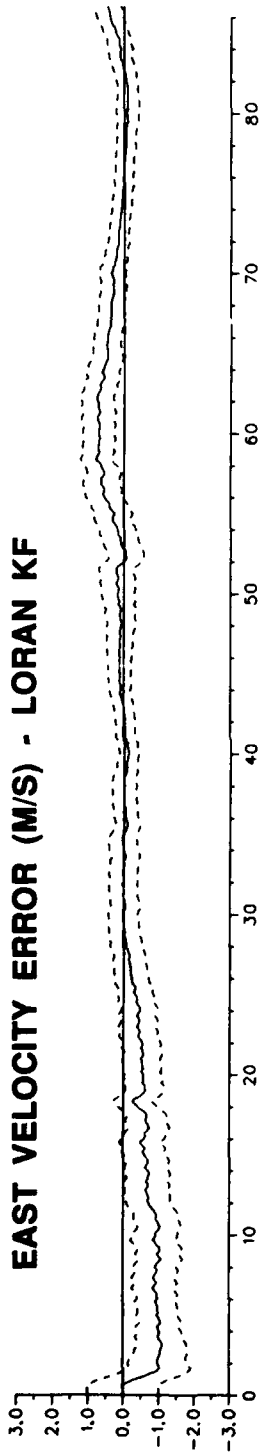
TIME (MINS.)

FLIGHT #1 DATA

FIG. 10: COMPARISON OF KF CONFIGURATIONS - NORTH VELOCITY ERRORS

FIG. 11: COMPARISON OF KF CONFIGURATIONS -
EAST VELOCITY ERRORS
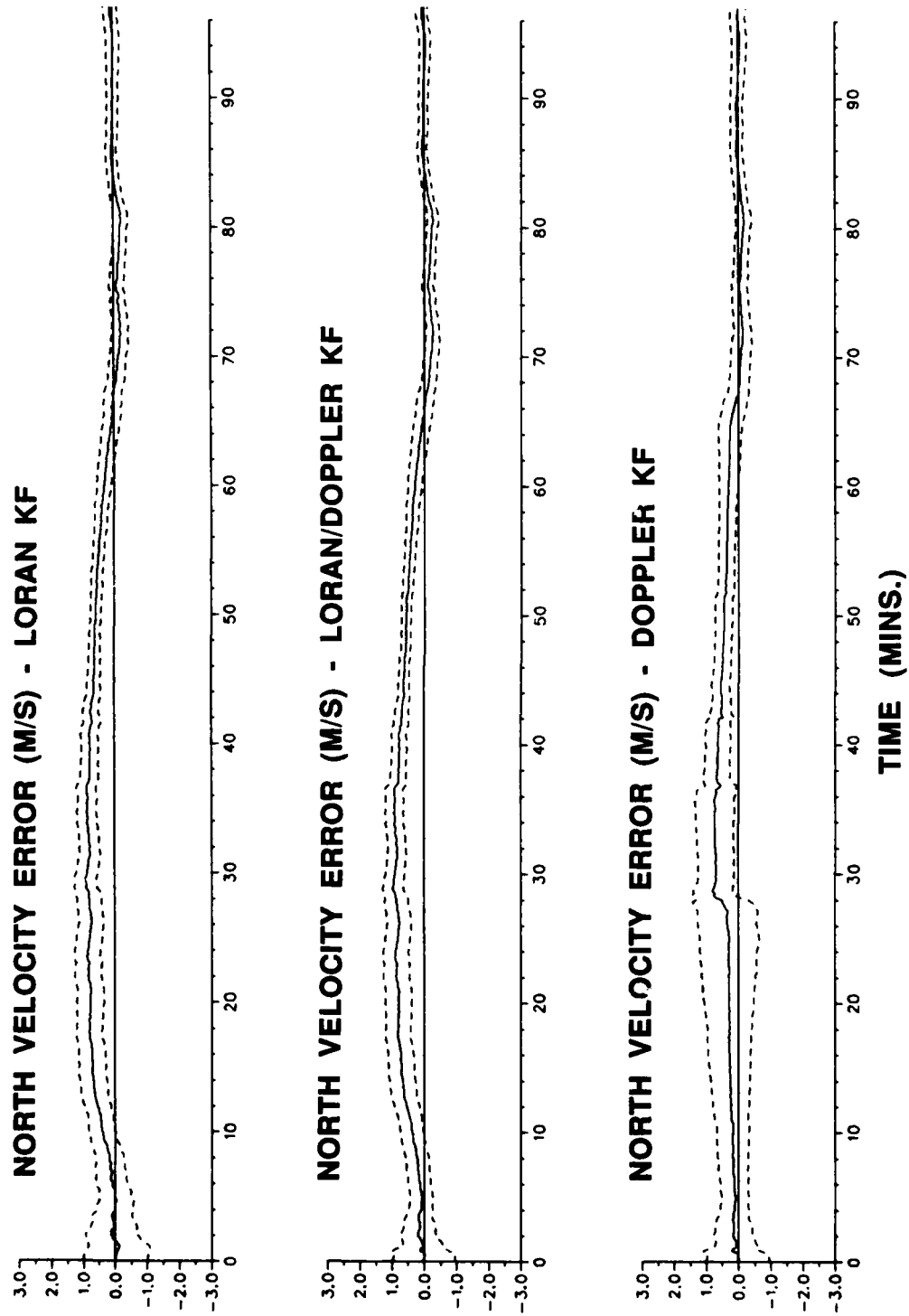
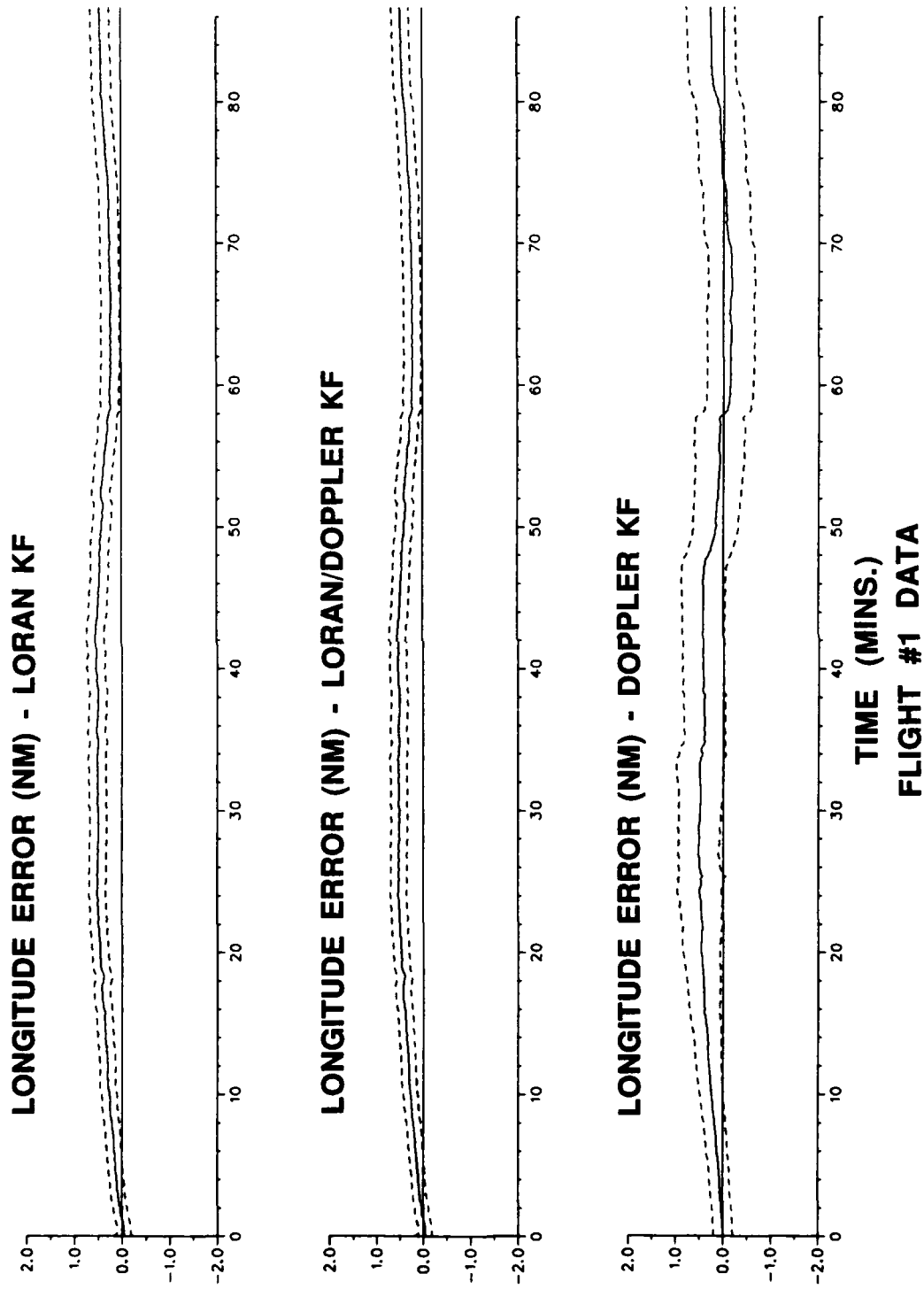FIG. 12: COMPARISON OF KF CONFIGURATIONS -
NORTH VELOCITY ERRORS
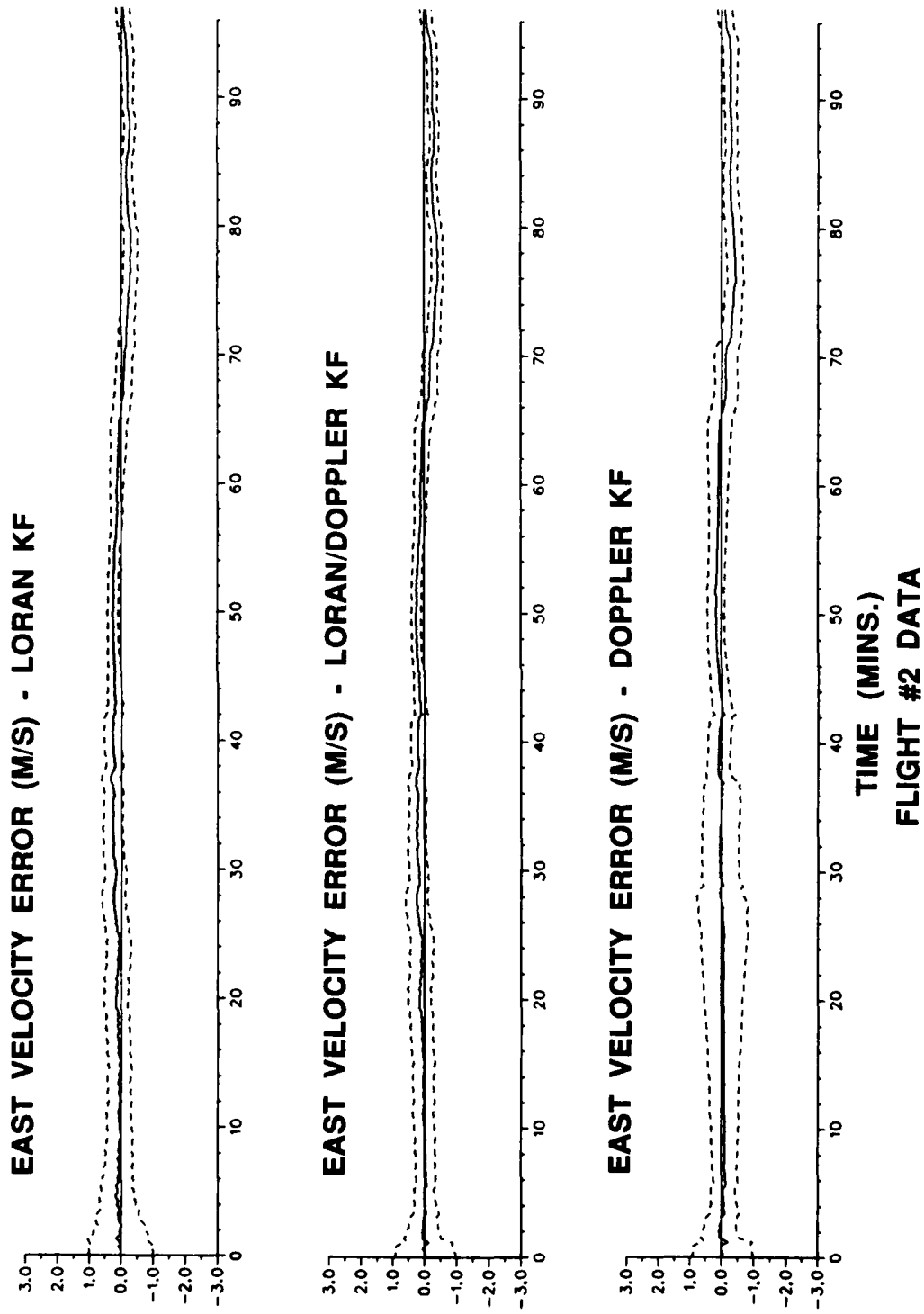
FIG. 13: COMPARISON OF KF CONFIGURATIONS -
EAST VELOCITY ERRORS
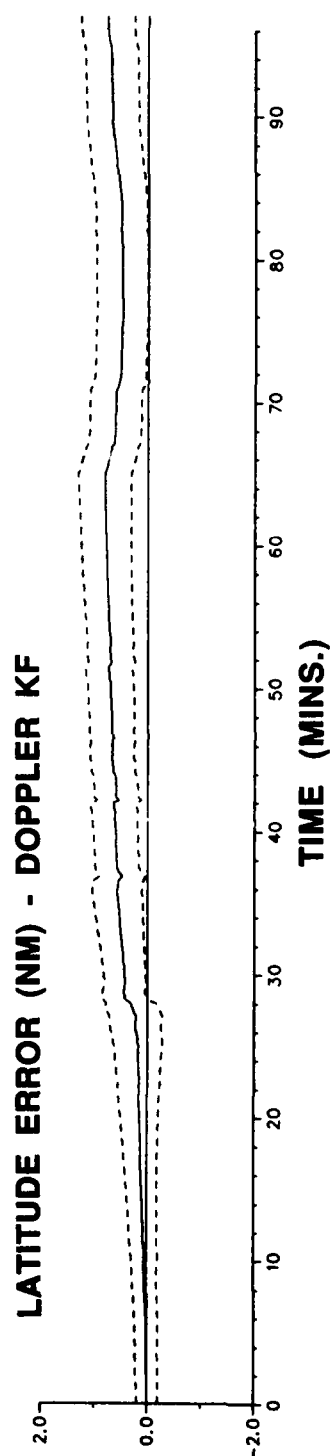
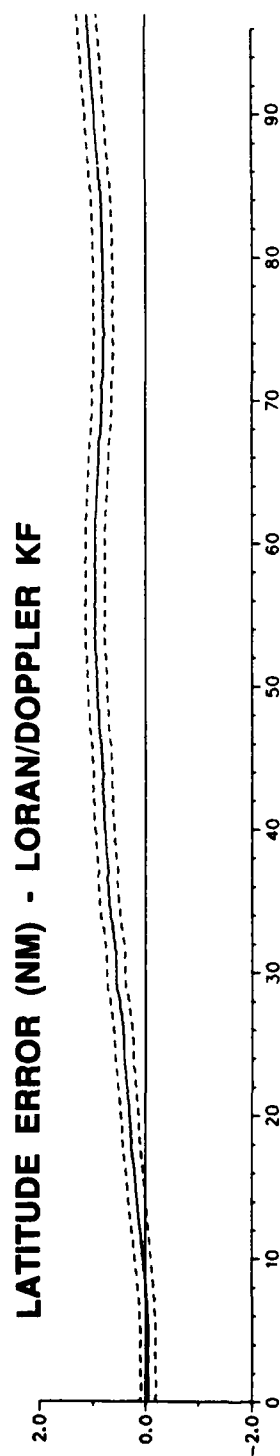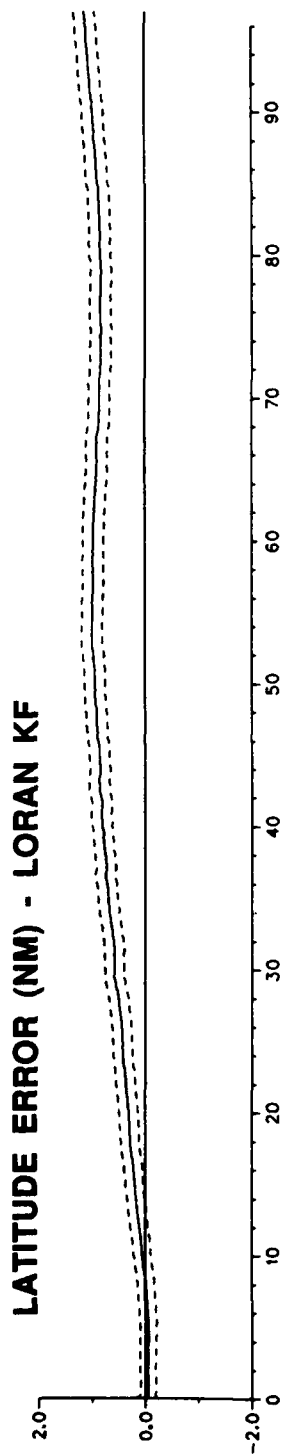FIG. 14: COMPARISON OF KF CONFIGURATIONS - LATITUDE ERRORS

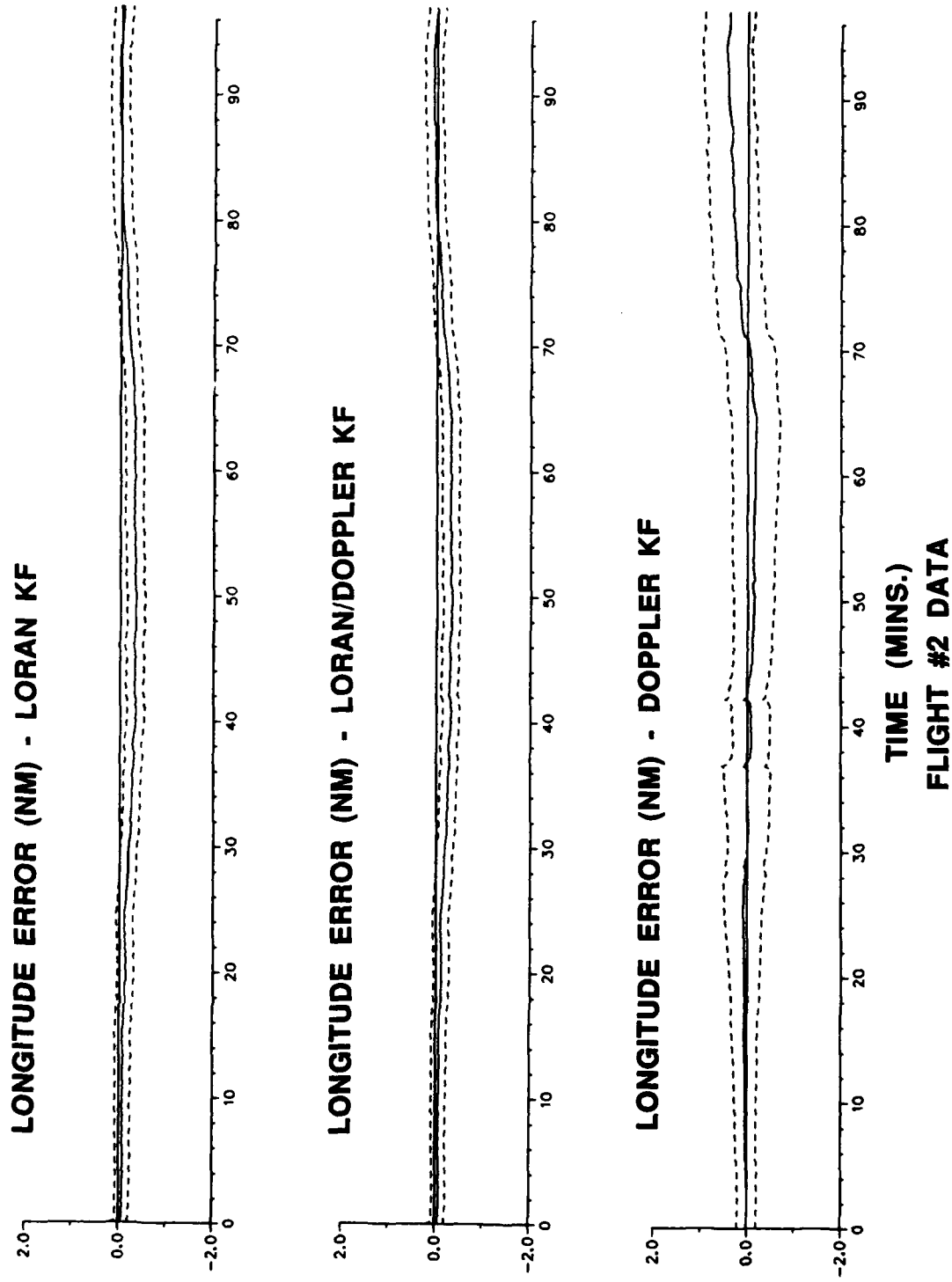FIG. 15: COMPARISON OF KF CONFIGURATIONS - LONGITUDE ERRORS

38

LATITUDE ERROR (NM) - LORAN KF

LATITUDE ERROR (NM) - LORAN/DOPPLER KF

LATITUDE ERROR (NM) - DOPPLER KF

TIME (MINS.)
FLIGHT #2 DATA

FIG. 16: COMPARISON OF KF CONFIGURATIONS - LATITUDE ERRORS

FIG. 17: COMPARISON OF KF CONFIGURATIONS - LONGITUDE ERRORS

REPORT DOCUMENTATION PAGE / PAGE DE DOCUMENTATION DE RAPPORT

REPORT/RAPPORT	REPORT/RAPPORT
NAE-AN-61 1a	NRC No. 31023 1b

REPORT SECURITY CLASSIFICATION CLASSIFICATION DE SÉCURITÉ DE RAPPORT Unclassified 2	DISTRIBUTION (LIMITATIONS) Unlimited 3

TITLE/SUBTITLE/TITRE/SOUS-TITRE

An Improved Airborne Wind Measurement Technique for the NAE Twin Otter

4

AUTHOR(S)/AUTEUR(S)

B.W. Leach and J.I. MacPherson

5

SERIES/SÉRIE

Aeronautical Note

6

CORPORATE AUTHOR/PERFORMING AGENCY/AUTEUR D'ENTREPRISE/AGENCE D'EXÉCUTION

National Research Council Canada
7 National Aeronautical Establishment   Flight Research Laboratory

SPONSORING AGENCY/AGENCE DE SUBVENTION

8

DATE 89-11 9	FILE/DOSSIER 10	LAB. ORDER COMMANDE DU LAB. 11	PAGES 44 12a	FIGS/DIAGRAMMES 17 12b

NOTES

13

DESCRIPTORS (KEY WORDS)/MOTS-CLÉS

  1. Airborne equipment   3. Twin Otter — Wind measurement
  2. Wind measurement
14

SUMMARY/SOMMAIRE

      Airborne wind measurement techniques currently being used onboard the NAE Twin Otter Atmospheric Research Aircraft are described and their fundamental limitations are discussed. In particular, a recently acquired LTR-90-100 strapdown inertial reference system (IRS) demonstrates significant low frequency Schuler oscillations in its velocity components (attaining peak errors of 2 to 3 mps), actually degrading wind computation accuracy compared with older techniques. A new wind measurement technique, based on a Kalman filter integrated navigation approach, is described which solves this problem and provides wind computation accuracy superior to previous methods. Preliminary results, based on applying the Kalman filter to Twin Otter flight test data, indicate that inertial velocity accuracies of 0.3 mps RMS (per channel) are atttainable, with a corresponding improvement in the accuracy of earth-referenced wind components.

15